Effective field theory of magnons: Chiral magnets and the Schwinger mechanism

Masaru Hongo [1,2] Toshiaki Fujimori,[3,4] Tatsuhiro Misumi,[5,4] Muneto Nitta,[3,4] and Norisuke Sakai [3,4]

[1]*Department of Physics, University of Illinois, Chicago, Illinois 60607, USA*
[2]*RIKEN iTHEMS, RIKEN, Wako 351-0198, Japan*
[3]*Department of Physics, Keio University, Yokohama 223-8521, Japan*
[4]*Research and Education Center for Natural Sciences, Keio University, Yokohama 223-8521, Japan*
[5]*Department of Mathematical Science, Akita University, Akita 010-8502, Japan*

We develop the effective field theoretical descriptions of spin systems in the presence of symmetry-breaking effects: the magnetic field, single-ion anisotropy, and Dzyaloshinskii-Moriya interaction. Starting from the lattice description of spin systems, we show that the symmetry-breaking terms corresponding to the above effects can be incorporated into the effective field theory as a combination of a background (or spurious) SO(3) gauge field and a scalar field in the symmetric tensor representation, which are eventually fixed at their physical values. We use the effective field theory to investigate mode spectra of inhomogeneous ground states, focusing on one-dimensionally noncollinear states, such as helical and spiral states. Although the helical and spiral ground states share a common feature of supporting the gapless Nambu-Goldstone modes associated with the translational symmetry breaking, they have qualitatively different dispersion relations: isotropic in the helical phase while anisotropic in the spiral phase. We clarify the reason for this qualitative difference based on the symmetry-breaking pattern. As another application, we discuss the magnon production induced by an inhomogeneous magnetic field, and find a formula akin to the Schwinger formula. Our formula for the magnon production gives a finite rate for antiferromagnets, and a vanishing rate for ferromagnets, whereas that for ferrimagnets interpolates between the two cases.

I. INTRODUCTION

Symmetry and its spontaneous breaking give one of the most fundamental concepts in modern physics. If the ground state exhibits a spontaneous breaking of continuous global symmetry of the system, the Nambu-Goldstone (NG) theorem predicts the inevitable appearance of the gapless excitation, or the NG mode [1–3]. In relativistic systems respecting the Lorentz symmetry, the number of broken global symmetries is matched with that of the NG modes while in nonrelativistic systems, it is, in general, not. Furthermore, in the latter case, dispersion relations of the resulting NG modes often show the quadratic behavior ($\omega = \pm a\mathbf{k}^2$) rather than the relativistic linear one ($\omega = \pm c|\mathbf{k}|$). Besides, the NG modes associated with spontaneous space-time symmetry breaking have several characteristic behaviors such as the anisotropic dispersion relation realized in, e.g., the smectic-A phase of liquid crystals [4–6] and the Fulde-Ferrell-Larkin-Ovchinnikov phase of superconductors [7–9], in addition to the mismatch between the numbers of broken symmetries and NG modes. Although these behaviors are beyond the prediction of the original NG theorem, recent theoretical developments clarify both the counting rule and dispersion relation of the NG mode associated with the internal symmetry breaking of nonrelativistic systems [10–25]. Also, there are several approaches to understand the NG modes for spontaneous space-time symmetry breaking [26–32]. One way to work out the nonrelativistic and spacetime generalization of the NG theorem is to use the effective field theory (EFT) (see, e.g., Refs. [11,18,20,22,29]).

Magnons, or quantized spin waves, in various kinds of magnets— antiferromagnets, ferromagnets, and ferrimagnets—give a canonical condensed matter example of these NG modes; a relativistic one in the antiferromagnets and a nonrelativistic one in the ferro/ferrimagnets. Although spin systems are originally described as lattice models, we can still describe their low-energy dynamics based on a continuum field theory at energy scales much lower than the inverse lattice spacing. We can regard this field theory model as an EFT of magnons that describes magnon dynamics at low energies [33–38]. In addition, the magnon EFT can incorporate various symmetry-breaking terms, such as a Zeeman term due to the coupling to external magnetic fields and single-ion anisotropy, as those terms are induced by small background fields that break symmetry explicitly (see, e.g., Ref. [38]). Thus, the spin system serves as one of the best places for investigating the nontrivial dynamics caused by the background field. An interesting symmetry-breaking term attracting much attention recently is the Dzyaloshinskii-Moriya (DM) [39,40] interaction that arises from the spin-orbit coupling in a specific class of magnets called chiral magnets. Another example is the inhomogeneous magnetic field, which may drastically change the dynamics of the magnon.

In lattice models, the DM interaction represents an interaction term proportional to the vector product of neighboring spins, which favors the easy-plane noncollinear ordering. As a result of the competition between the DM interaction and

the Zeeman term or the anisotropic term in the potential, a lot of interesting noncollinear ground states appear, such as the chiral soliton lattice in a $(1 + 1)$-dimensional spin chain and a skyrmion lattice in $(2 + 1)$-dimensional spin systems, whose peculiar thermodynamic and transport behaviors have been recently observed [41–47]. Recent theoretical studies in the presence of the DM interaction have revealed various Bogomol'ny-Prasad-Sommerfield [48,49] (BPS) solutions [50–54] and instanton solutions [55], which enable us to study chiral magnets analytically to some extent. When the DM interaction is more influential than the terms in the potential, spin systems tend to realize simple noncollinear ground states where the magnetization vector is modulated along one dimension. We call this one-dimensionally modulated ground state a helical state (see, e.g., Ref. [55]) or spiral state [56], depending on the direction of the DM interaction relative to the potential terms. In terms of the magnetization vector $\boldsymbol{n} = (n^1, n^2, n^3)$ with a constraint $\boldsymbol{n} \cdot \boldsymbol{n} = 1$, we can represent the Zeeman term and the single-ion anisotropy term as terms in the potential linear and quadratic in the third component of magnetization vector n^3. If we take the DM interaction as an interaction term between n^1 and n^2 of spins in neighboring lattice sites, we find that the ground state is the helical state, provided the anisotropy term in the potential does not favor easy-axis strongly [55]. If we take the DM interaction as an interaction term between n^3 and n^1, n^2 of spins at neighboring lattice sites, we find the spiral state as the ground state, provided potential terms are not too strong [56].

Thanks to its low-dimensional character, it is much simpler to analyze the low-energy dynamics in the helical and spiral phases than other possible noncollinear ground states. Since both the helical and spiral phases show the one-dimensional noncollinear order, we can expect that they share an essential property: for instance, one may expect both of them to support the phonon as the NG mode associated with the spontaneous breaking of translational symmetry. Nevertheless, we need to be careful since a general statement of the NG theorem is absent in the case of spontaneous breaking of the space-time symmetry. It is worth studying the number of massless degrees of freedom and dispersion relation of these modes in each case. To study the energy spectrum, previous works rely on, e.g., the linear spin wave theory [57–61], the time-dependent Ginzburg-Landau theory [62], and the effective Hamiltonian [63] (see also Ref. [64] for a review).

In this paper, we study the dynamics of spin systems by means of EFT, focusing on physical effects induced by explicit symmetry-breaking terms; namely, the magnetic field, single-ion anisotropy, and the DM interaction. Starting from the lattice description of spin systems with these symmetry-breaking terms, we can incorporate them into the EFT by treating them as background fields on which the SO(3) transformation for the magnetization vector acts appropriately. We find that the DM interaction can be described by a background SO(3) gauge field [53] and the magnetic field can be described by the temporal component of SO(3) gauge field, whereas a scalar field in the symmetric rank-two tensor representation is needed to describe the single-ion anisotropy (see, e.g., Ref. [38]). The assignment of the (spurious) gauge transformation rules to these background (spurious) fields helps to incorporate explicit breaking terms into the EFT of spin systems.

This symmetry-based construction of the EFT with the DM interaction provides a unified description of magnons in antiferromagnets, ferromagnets, and ferrimagnets with the DM interaction.

We present several applications of our EFT of magnons. First, we investigate the low-energy dynamics induced by the DM interaction. A simple choice of the DM interaction gives the helical ground state and another choice gives the spiral ground state. Both of these noncollinear ground states spontaneously break the translation symmetry along one direction. While both helical and spiral ground states support gapless NG modes, their properties are qualitatively different: the NG mode in the helical phase shows the isotropic linear dispersion relation, whereas that in the spiral phase shows the anisotropic dispersion relation (see, e.g., Refs. [57–59,62–64] for previous works on the anisotropic dispersion relation). Moreover, the dispersion relation of the NG mode in the spiral phase is sensitive to the types of magnets (antiferromagnets, ferromagnets, or ferrimagnets) though that in the helical phase is not. The spiral state in an antiferromagnet shows a linear dispersion along the modulation and a quadratic dispersion perpendicularly. On the other hand, spiral states in ferromagnets and ferrimagnets show quadratic dispersions along the modulation and quartic dispersions perpendicularly. We clarify the reason why these differences arise from the symmetry-based EFT viewpoint along the line of Refs. [11,18,20,22,29].

As another application, we investigate the production rate of magnons caused by the inhomogeneous magnetic field from the collinear ground state. We show the magnon EFT with easy-axis anisotropy can be mapped into a relativistic model of a charged scalar field whose gap is determined by the sum of the easy-axis potential and the ratio of magnetization and condensation parameter f_t^2. We obtain a formula for the production rate of magnons analogous to Schwinger's formula [65–68] (or the Landau-Zener formula [69–72]) for the charged particle pair production rate by a constant electric field. Our formula shows that the antiferromagnet corresponds to the relativistic regime (small effective mass) and gives the nonvanishing magnon production rate, whereas the ferromagnet corresponds to the nonrelativistic regime (infinite effective mass) and gives the vanishing production rate. The production rate for ferrimagnets interpolates between those for antiferromagnets and ferromagnets.

The paper is organized as follows. In Sec. II, we describe a way to implement symmetry-breaking terms in EFT starting from spin systems on a lattice. In Sec. III, we write down an EFT of magnons in the form of the O(3) nonlinear sigma model and confirm the known result for the noncollinear ground state. In Sec. IV, we apply our EFT to the helical/spiral ground states induced by the DM interaction. In Sec. V, we apply our EFT to describe the production of magnons by an inhomogeneous magnetic field. Section VI is devoted to a discussion. In the Appendix, we present a coset construction of EFT for NG modes.

II. MODEL AND SYMMETRY ON LATTICE

Let us consider spin systems whose SO(3) spin-rotation symmetry is explicitly but softly broken due to the external
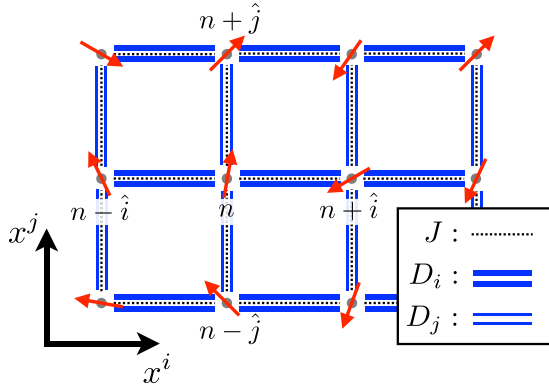
FIG. 1. A schematic picture of the spin system under consideration. We assume the localized spins live on the cubic-type lattice.

magnetic field, DM interaction, and single-ion anisotropic interaction terms. As a concrete example, we consider spin systems, whose Hamiltonian reads[1]

$$\hat{H} = \sum_n \sum_{i=1}^d \left[\frac{|J|}{2} (\hat{s}^{n+\hat{i}} - \mathrm{sgn}(J)\hat{s}^n)^2 + \boldsymbol{D}_i \cdot (\hat{s}^n \times \hat{s}^{n+\hat{i}}) \right]$$
$$- \sum_n [\mu\boldsymbol{B} \cdot \hat{s}^n + (\hat{s}^n)^t C \hat{s}^n]$$
$$= -\sum_n \sum_{i=1}^d (J\delta^{ab} + D_i^c \epsilon_c^{ab}) \hat{s}_a^n \hat{s}_b^{n+\hat{i}}$$
$$- \sum_n [\mu B^a \hat{s}_a^n + C^{ab} \hat{s}_a^n \hat{s}_b^n] + (\text{const}), \qquad (1)$$

where $\hat{s}^n$ denotes a spin vector on site n with the (anti)ferromagnetic interaction $J > 0 \, (J < 0)$, $\mu\boldsymbol{B}$ the external magnetic field $\boldsymbol{B}$ multiplied by the magnetic moment μ, the DM interaction $\boldsymbol{D}_i$, and anisotropic interaction C known as the single-ion anisotropy. On the second line, we have introduced the Kronecker delta δ^{ab} and the Levi-Civita symbol ϵ^{abc} for the internal spin indices $a, b, \dots = 1, 2, 3$, and the summation over the repeated indices is implied. To express the nearest-neighbor pairs, we defined the direction $\hat{i} = 1, 2, \dots, d$ with a spatial dimension d. In this paper, we only consider the simple cubic-type lattice schematically shown in Fig. 1, where the frustration in the antiferromagnetic case does not appear.[2] In addition, when considering the antiferromagnetic order, we focus on the G-type antiferromagnet, in which the Néel order appears along all the spatial directions. Relax-

---

[1]The expression in the first line of this equation is useful when we explicitly consider the continuum limit. This is because a relation between a continuum order parameter field and a lattice spin vector depends on whether the system shows ferromagnetic or antiferromagnetic order controlled by the sign of J.

[2]The DM interaction in real materials appears if the inversion symmetry is broken—e.g., in spin systems on the Kagome lattice or on the cubic lattice with a distortion (see, e.g., Refs. [116,117]). Thus, one may regard our simplification as just a theoretical one or assume the presence of the inversion breaking point in another spatial direction where the spin does not stay.

ing these assumptions is an interesting problem but beyond the scope of the present paper. Here the DM interaction $\boldsymbol{D}_i$ is assumed to have a directional dependence expressed by its subscript i.

In the absence of explicit symmetry-breaking terms ($D_i^c = \mu B^a = C^{ab} = 0$), the Hamiltonian enjoys SO(3) symmetry, whose possible spontaneous breaking leads to the gapless collective excitations, or magnons (quantized spin wave) as NG modes. By promoting the symmetry-breaking parameters to background fields (spurions), we can construct a low-energy effective Lagrangian for the magnons with other possible low-energy modes based only on the symmetry argument [38]. Although the explicit breaking terms break the global SO(3) symmetry, we can investigate their effects using the background field (or the so-called spurion) method if they are small compared to the symmetric interaction ($|D_i^c|$, $|\mu B^a|$, $|C^{ab}| \ll |J|$).

As the first attempt to parametrize the DM interaction, let us introduce the SO(3) gauge field coupled to the Noether current corresponding to the global SO(3) symmetry. When the Hamiltonian is given only by the first term in Eq. (1), $\hat{H}_0 \equiv -\sum_{n,i} J(\hat{s}^n)^t \hat{s}^{n+\hat{i}} + (\text{const})$, the Heisenberg equation of motion for $\hat{s}_a^n$ generated by the SO(3) invariant Hamiltonian $\hat{H}_0$ provides a discretized version of the conservation law of the Noether current:

$$\partial_t \hat{J}_a^0(n) + \sum_{i=1}^d [\hat{J}_a^i(n+\hat{i}/2) - \hat{J}_a^i(n-\hat{i}/2)] = 0$$
$$\text{with} \quad \begin{cases} \hat{J}_a^0(n) \equiv \hat{s}_a^n \\ \hat{J}_a^i(n+\hat{i}/2) = J\epsilon_a^{bc} \hat{s}_b^n \hat{s}_c^{n+\hat{i}}. \end{cases} \qquad (2)$$

By introducing the background gauge field coupled to the Noether current, we obtain the following modification of the Hamiltonian:

$$\hat{H}_0 \rightarrow \hat{H}_0 - \sum_n \sum_{i=1}^d a A_i^a(n+\hat{i}/2) \hat{J}_a^i(n+\hat{i}/2)$$
$$- \sum_n A_0^a(n) \hat{J}_a^0(n)$$
$$= -\sum_n \sum_{i=1}^d [J\delta^{ab} + Ja A_i^c(n+\hat{i}/2)\epsilon_c^{ab}] \hat{s}_a^n \hat{s}_b^{n+\hat{i}}$$
$$- \sum_n A_0^a(n) \hat{s}_a^n, \qquad (3)$$

with an SO(3) gauge field $A_\mu^a \, (a = 1, 2, 3)$. Here we introduced the lattice spacing ℓ between spins for future convenience. We can now identify two symmetry-breaking terms μB^a and D_i^a in the original Hamiltonian in Eq. (1) as the following background values of the SO(3) gauge field:

$$A_0^a(n) \equiv \mu B^a, \quad A_i^a(n+\hat{j}/2) \equiv (J\ell)^{-1} D_i^a. \qquad (4)$$

Although this illustrates the basic idea of the background field (spurion) method for the magnetic field and the DM interaction term, this simplified Noether procedure in Eq. (3)

does not implement the local SO(3) gauge invariance fully on the lattice and is *not* complete.

To correctly implement the SO(3) gauge invariance on the lattice, we draw an analogy to the Hamiltonian lattice gauge theory [73]. We first make the Hamiltonian $\hat{H}_0$ invariant under the local SO(3) transformation,

$$\hat{H}_0 \to \hat{H}_0' \equiv \sum_n \sum_{i=1}^d \frac{|J|}{2} [U(n, n+\hat{i})\hat{\mathfrak{s}}^{n+\hat{i}} - \mathrm{sgn}(J)\hat{\mathfrak{s}}^n]^2 \\ - \sum_n [\boldsymbol{A}_0(n)]^t \hat{\mathfrak{s}}^n, \tag{5}$$

where the local SO(3) transformation $g(n) \in$ SO(3) acts on $\hat{\mathfrak{s}}^n$, $U(n, n+\hat{i})$, and $\boldsymbol{A}_0$ as

$$\hat{\mathfrak{s}}^n \to g(n)\hat{\mathfrak{s}}^n \\ U(n, n+\hat{i}) \to g(n)U(n, n+\hat{i})g(n+\hat{i})^t \\ \boldsymbol{A}_0(n) \to g(n)\boldsymbol{A}_0. \tag{6}$$

The link variable $U(n, n+\hat{i})$ corresponds to a spatial part of the SO(3) gauge field on the lattice (see, e.g., Ref. [73] in detail). We will eventually identify its continuum limit describing the DM interaction. Noting that the last transformation is equivalent to $A_0(n) \equiv A_0^a(n)t_a \to g(n)A_0 g^t(n)$, which is identified as a time-independent gauge transformation, we will further consider time-dependent gauge invariance acting on $A_0(t, n)$ as[3]

$$A_0(t, n) \to g(t, n)A_0(t, n)g(n, t)^t + ig(t, n)^{-1}\partial_0 g(n, t)^t. \tag{7}$$

We now study the expansion in powers of the lattice spacing a of the gauge-invariant theory Eq. (5) to obtain the original Hamiltonian in Eq. (1) with symmetry-breaking terms μB^a, D_i^a, and C^{ab}, ignoring higher-order terms in powers of a, which will become irrelevant in the continuum limit. By expanding the link variable U at a small lattice spacing a, we can identify the SO(3) gauge field A_i^a as

$$U(n, n+\hat{i}) = e^{iaA_i^a(n+\hat{i}/2)t_a} \\ = I_{3\times 3} + i\ell A_i^a(n+\hat{i}/2)t_a + O(\ell^2). \tag{8}$$

Counting $\hat{\mathfrak{s}}^{n+\hat{i}} + \mathrm{sgn}(J)\hat{\mathfrak{s}}^n = O(\ell)$, the $O(\ell^2)$ term in U gives higher-order terms which vanish in the continuum limit. Here, we have also introduced generators of the Lie algebra $t_a \in$ SO(3) satisfying

$$[t_a, t_b] = i\epsilon_{ab}^c t_c. \tag{9}$$

---

[3]We can rigorously justify this treatment as follows: With the $\mathbb{C}\mathrm{P}^1$ parametrization of the spin with $z_n = (z_n^1, z_n^2)^t$, the path-integral formula gives the Lagrangian $\mathcal{L} = \sum_n iz_n^\dagger \partial_0 z_n - H(sz^\dagger \boldsymbol{\sigma} z) = \sum_n iz_n^\dagger D_0 z_n - H_0(sz^\dagger \boldsymbol{\sigma} z) + \sum_n \sum_{i=1}^d A_i^a J_a^i$. The first term with single time derivative is the so-called Berry phase term. We also introduced a covariant derivative $D_0 z_n \equiv \partial_0 z_n - isA_0^a \sigma_a z_n$ (corresponding to SO(3), due to the redundancy of the U(1) part $z_n \to e^{i\theta(x)}z_n$). Thus, the $A_0^a \hat{\mathfrak{s}}^n$ term in the Hamiltonian comes from the correct gauging of the temporal part of SO(3) symmetry.

Using the explicit form of t_a in the vector representation,

$$t_1 = \begin{pmatrix} 0 & 0 & 0 \\ 0 & 0 & -i \\ 0 & i & 0 \end{pmatrix}, \quad t_2 = \begin{pmatrix} 0 & 0 & i \\ 0 & 0 & 0 \\ -i & 0 & 0 \end{pmatrix}, \\ t_3 = \begin{pmatrix} 0 & -i & 0 \\ i & 0 & 0 \\ 0 & 0 & 0 \end{pmatrix}, \tag{10}$$

we expand the gauge-invariant Hamiltonian in powers of the lattice spacing ℓ as

$$\hat{H}_0' = \sum_n \sum_{i=1}^d \frac{|J|}{2} [\hat{\mathfrak{s}}^{n+\hat{i}} - \mathrm{sgn}(J)\hat{\mathfrak{s}}^n + i\ell A_i^a t_a \hat{\mathfrak{s}}^{n+\hat{i}} + O(\ell^2)]^2 \\ - \sum_n \boldsymbol{A}_0 \cdot \hat{\mathfrak{s}}_a^n \\ = \sum_n \sum_{i=1}^d \left[\frac{|J|}{2}(\hat{\mathfrak{s}}^{n+\hat{i}} - \mathrm{sgn}(J)\hat{\mathfrak{s}}^n)^2 + J\ell \boldsymbol{A}_i \cdot (\hat{\mathfrak{s}}^{n+\hat{i}} \times \hat{\mathfrak{s}}^n) \right] \\ - \sum_n \left[\boldsymbol{A}_0 \cdot \hat{\mathfrak{s}}_a^n - \frac{|J|\ell^2}{2}(\hat{\mathfrak{s}}^n)^t (A_i^a t_a)^2 \hat{\mathfrak{s}}^n \right], \tag{11}$$

where we have not explicitly displayed terms that vanish in the naive continuum limit [$(O(J\ell^3)$ terms]. Comparing this with the original Hamiltonian Eq. (1), we can confirm the identification Eq. (4) of the background values of the fields to obtain the magnetic field μB and the DM interaction D_i^a, together with a specific value C_{cr} of the anisotropic potential [the last term C in Eq. (1)], given by

$$C_{\mathrm{cr}} = -\frac{|J|\ell^2}{2}(A_i^a t_a)^2 = -\frac{1}{2|J|}(D_i^a t_a)^2. \tag{12}$$

This fine-tuned potential corresponds to the case of the continuum Hamiltonian whose potential can be combined with the DM interaction simply as the square of the covariant derivative.

The generic values of the single-ion anisotropy C can also be implemented by introducing another background scalar field $W(n)$ in the symmetric rank-two tensor representation, on which the local SO(3) transformation $g(n)$ acts as $W(n) \to g(n)W(n)g(n)^t$. We should identify its background value as

$$W(n) \equiv C - C_{\mathrm{cr}}. \tag{13}$$

Thus, apart from higher-order terms in powers of the lattice spacing a, which vanish in the naïve continuum limit, we find that the Hamiltonian in Eq. (1) with symmetry-breaking terms μB^a, D_i^a, and C^{ab} can be obtained from the lattice gauge invariant theory,

$$\hat{H}_0'' \equiv \sum_n \sum_{i=1}^d \frac{|J|}{2} [U(n, n+\hat{i})\hat{\mathfrak{s}}^{n+\hat{i}} - \mathrm{sgn}(J)\hat{\mathfrak{s}}^n]^2 \\ - \sum_n A_0^a(n)\hat{\mathfrak{s}}_a^n - \sum_n (\hat{\mathfrak{s}}^n)^t W(n)\hat{\mathfrak{s}}^n, \tag{14}$$

at particular values of the background gauge field A_0, A_i and scalar field W given in Eqs. (4) and (13).

III. EFFECTIVE FIELD THEORY OF MAGNONS

In this section, we implement explicit symmetry-breaking terms presented in the previous section into a field-theoretical description of spin systems, or the O(3) nonlinear sigma model. We also clarify the matching condition for the low-energy coefficient in the collinear (homogeneous) ground state and review the low-energy spectrum in the absence of the explicit symmetry breaking (also see the Appendix for a coset construction as a complementary way to derive the effective Lagrangian).

A. O(3) nonlinear sigma model description

Since we are interested in the low-energy (long wavelength) behaviors of the system, we can employ the field-theoretical (continuum) description of the system. A continuum field-theoretical description of magnons (spin waves) is given by the O(3) nonlinear sigma model, in which a three-component unit vector $\boldsymbol{n} = (n^1, n^2, n^3)^t$ with $n^a n_a = 1$ plays a role as a dynamical degree of freedom. We note that this unit vector expresses the usual magnetization order parameter in the ferromagnetic case, while it represents the Néel order parameter in the antiferromagnetic case.

The local SO(3) transformation simply acts on the vector field $\boldsymbol{n}$ as $\boldsymbol{n} \to g(x)\boldsymbol{n}$ with $g(x) \in$ SO(3), as is the case with the lattice spin. The symmetry-based discussion in the previous section enables us to incorporate explicit breaking terms in the O(3) nonlinear sigma model. In fact, taking the continuum limit of the background (spurious) gauge and scalar fields introduced in the previous section, we have the SO(3) gauge field $A_\mu(x) \equiv A_\mu(x)^a t_a$ and the scalar $W(x)$ in the symmetric tensor representation on which the local SO(3) transformation $g(x) \in$ SO(3) acts as

$$A_\mu(x) \to g(x)A_\mu(x)g^{-1}(x) + ig(x)\partial_\mu g^{-1}(x)$$
$$W(x) \to g(x)W(x)g^{-1}(x). \tag{15}$$

Using these, we construct the general local SO(3) invariant effective Lagrangian and eventually fix the (spurious) fields to the nontrivial background values as

$$A_0^a(x) = \mu B^a,$$
$$A_i^a(x) = (J\ell)^{-1}D_i^a \equiv \kappa_i^a, \tag{16}$$
$$W(x) = C - C_{\text{cr}},$$

to investigate small effects of the explicit breaking terms in the lattice Hamiltonian Eq. (1).

Using the transformation rules of the fields $n^a(x)$, $A_\mu^a(x)$, and $W(x)$ as ingredients, we can construct the general SO(3) invariant effective Lagrangian. In the leading order of the derivative expansion, where we only keep terms up to second order in derivatives, the SO(3) invariant effective Lagrangian is given by

$$\mathcal{L}_{\text{eff}} = \frac{m(n^2\partial_0 n^1 - n^1\partial_0 n^2)}{1 + n^3} + mA_0^a n_a$$
$$+ \frac{f_t^2}{2}(D_0 n^a)^2 - \frac{f_s^2}{2}(D_i n^a)^2 + rW^{ab}n_a n_b, \tag{17}$$

where we defined a covariant derivative with the SO(3) background gauge field as

$$D_\mu n^a \equiv \partial_\mu n^a - \epsilon^a_{bc} n^b A_\mu^c. \tag{18}$$

Equation (17) supplemented with Eqs. (16) defines our EFT for general magnets, including chiral magnets. This continuum field theory should be valid at low energies and contains four parameters m, f_t, f_s, and r as low-energy coefficients. They can be determined from the underlying lattice model by the matching condition, which will be discussed shortly. Note that the sum of the first and second terms in Eq. (17) manifestly breaks the Lorentz invariance[4] with an effective speed of light $c_s \equiv f_s/f_t$, but is SO(3) gauge invariant [15]. If the symmetry-breaking terms vanish ($A_\mu^a = 0$, $W^{ab} = 0$), the effective Lagrangian in Eq. (17) reduces to the usual O(3) nonlinear sigma model describing ferromagnets ($m \neq 0$, $f_t = 0$), antiferromagnets ($m = 0$, $f_t \neq 0$), and ferrimagnets ($m \neq 0$, $f_t \neq 0$). The first term is responsible for the quadratic gapless dispersion relation of the magnon in ferro/ferrimagnets. In the rest of this section, we will introduce the matching condition and study the low-energy spectrum on the top of the collinear ordered phase.

B. Matching condition and low-energy spectrum in collinear order

Before discussing magnon dynamics in the presence of symmetry-breaking terms, we here clarify the matching condition for low-energy coefficients m, f_t, f_s and r in the collinear ground state, which breaks approximate SO(3) symmetry. We also demonstrate the low-energy spectrum of gapless magnons in the absence of symmetry-breaking terms.

To illustrate the procedure in a simple context, let us assume that the symmetry-breaking background fields give the collinear ground state with the magnetization/Néel vector pointing the north pole as $\langle \boldsymbol{n} \rangle = \boldsymbol{n}_0 \equiv (0, 0, 1)^t$. We then introduce magnon fields π^α ($\alpha = 1, 2$) as fluctuations on the top of the ground state, which parametrize the vector $\boldsymbol{n}$ as

$$\boldsymbol{n} = (\pi^1, \pi^2, \sqrt{1 - (\pi^\alpha)^2})^t, \tag{19}$$

where we explicitly solved the constraint $n_a n^a = 1$. Substituting this parametrization into Eq. (17), we obtain the effective Lagrangian of magnons given by

$$\begin{aligned}
\mathcal{L}_{\text{eff}}^{(2)} = {}&-\frac{m}{2}\epsilon^3_{\alpha\beta}\pi^\alpha\partial_0\pi^\beta + m\left(\delta_a^3 + \delta_a^\alpha\pi_\alpha - \frac{1}{2}\delta_a^3(\pi^\alpha)^2\right)A_0^a \\
&+ rW^{33} + \frac{f_t^2}{2}\left[(D_0\pi^\alpha)^2 + \left(A_0^\alpha\pi_\alpha\right)^2\right] \\
&- \frac{f_s^2}{2}\left[(D_i\pi^\alpha)^2 + \left(A_i^\alpha\pi_\alpha\right)^2\right] \\
&+ r[(W^{13} + W^{31})\pi^1 + (W^{23} + W^{32})\pi^2] \\
&+ r[(W^{11} - W^{33})(\pi^1)^2 + (W^{22} - W^{33})(\pi^2)^2 \\
&+ (W^{12} + W^{21})\pi^1\pi^2] + \mathcal{L}_{\text{int}}, \tag{20}
\end{aligned}$$

---

[4]More precisely, a modified Lorentz symmetry remains exact, see Refs. [118–120].

where $\mathcal{L}_{\mathrm{int}}$ contains more than two magnon fields representing interactions between them. We have also defined the covariant derivative of the magnon field as

$$D_\mu \pi^\alpha = \partial_\mu \pi^\alpha + \epsilon_\beta^{3\alpha} A_\mu^\beta - A_\mu^3 \epsilon_{\beta 3}^\alpha \pi^\beta. \tag{21}$$

Since the ground state spontaneously breaks the SO(3) symmetry down to its subgroup SO(2)$_z$, the magnon fields can be identified as the NG bosons. The effective Lagrangian Eq. (20) is reparametrized by π^α fields to make their role as NG bosons manifest, and is equivalent to the original EFT in Eq. (17), provided all order terms of π^α in $\mathcal{L}_{\mathrm{int}}$ are kept. In the rest of this section, we assume symmetry-breaking terms in Eq. (20) do not induce a tachyonlike instability around the assumed ground state $\boldsymbol{n}_0 \equiv (0, 0, 1)^t$. Thus, the actual values of the symmetry-breaking terms in Eq. (20) cannot be arbitrary.

We now discuss the matching conditions within a tree-level analysis to fix the phenomenological parameters in the effective Lagrangian Eq. (20): the four parameters m, f_{t}, f_{s}, and r. We first introduce the SO(3) current defined by the variation of the effective action $\mathcal{S}$ in terms of the SO(3) gauge fields:

$$J_a^\mu(x) = \frac{\delta \mathcal{S}[\pi^\alpha; A_\mu^a, W]}{\delta A_\mu^a(x)}, \quad \mathcal{S}[\pi^\alpha; A_\mu^a, W] = \int d^{d+1}x \, \mathcal{L}_{\mathrm{eff}}. \tag{22}$$

Based on the derived effective Lagrangian, we specify the SO(3) spin currents in the expansion with respect to the magnon field $\pi^\alpha(x)$ as

$$\begin{aligned}
J_3^0 &\simeq m - \frac{m}{2}(\pi^\alpha)^2 \\
&\quad - f_{\mathrm{t}}^2 \epsilon_{\alpha \beta 3} \pi^\beta \big(\partial_0 \pi^\alpha + \epsilon_\gamma^{3\alpha} A_0^\gamma - A_0^3 \epsilon_{\gamma 3}^\alpha \pi^\gamma\big), \\
J_3^i &\simeq f_{\mathrm{s}}^2 \delta^{ij} \epsilon_{\alpha \beta 3} \pi^\beta \big(\partial_j \pi^\alpha + \epsilon_\gamma^{3\alpha} A_j^\gamma - A_j^3 \epsilon_{\gamma 3}^\alpha \pi^\gamma\big), \\
J_\alpha^0 &\simeq m\pi_\alpha - f_{\mathrm{t}}^2 \epsilon_{\alpha\beta}^3 \big(\partial_0 \pi^\beta + \epsilon_\gamma^{3\beta} A_0^\gamma - A_0^3 \epsilon_{\gamma 3}^\beta \pi^\gamma\big), \\
J_\alpha^i &\simeq f_{\mathrm{s}}^2 \delta^{ij} \epsilon_{\alpha\beta}^3 \big(\partial_j \pi^\beta + \epsilon_\gamma^{3\beta} A_j^\gamma - A_j^3 \epsilon_{\gamma 3}^\beta \pi^\gamma\big). \tag{23}
\end{aligned}$$

Here we only collect the leading-order terms with the magnon field π_α (J_α^0 and J_α^i also have terms quadratic with respect to the magnon field). Note that one magnon contribution appears in the currents J_α^μ for the broken symmetry while it does not in the current J_3^μ for the unbroken symmetry. It is also worth noting that there is zero-magnon contribution in J_3^0 for the ferro/ferrimagnetic case, which will lead to the matching condition specified below.

We then define the generating functional $Z[A_\mu^a, W]$ for the SO(3) current J_a^μ by the path integral over $\pi^\alpha(x)$:

$$Z[A_\mu^a, W] = \int \mathcal{D}\pi^\alpha \, \exp\big(i\mathcal{S}[\pi^\alpha; A_\mu^a, W]\big). \tag{24}$$

The expectation values of the currents can be obtained by taking the functional derivative with respect to A_μ^a:

$$\langle J_a^\mu(x) \rangle = i^{-1} \frac{\delta}{\delta A_\mu^a(x)} \ln Z[A_\mu^a, W]. \tag{25}$$

We can also introduce the generalized susceptibility for the SO(3) symmetry (correlation functions of current operators),

defined by

$$\chi_{ab}^{\mu\nu}(\omega, \boldsymbol{k}) = -\int d^{d+1}x \, e^{i\omega t - i\boldsymbol{k}\cdot\boldsymbol{x}} \frac{\delta^2 \ln Z[A_\mu^a, W]}{\delta A_\mu^a(x)\delta A_\nu^b(0)}. \tag{26}$$

If we wish to find the expectation values of the current operators and the susceptibility at the tree level, we just need to evaluate Eq. (24) at the collinear ground state $\pi^\alpha(x) = 0$ and the background values of A_μ^a and $W(x)$. Denoting the ground-state expectation value of an operator O by $\langle O \rangle$, we obtain the expectation value of the current operator $\hat{J}_a^\mu$ and the correlation functions of the current operators (susceptibility) at the tree-level approximation as

$$\begin{aligned}
\langle J_3^0(x) \rangle|_{\pi=0} &= m \\
\chi_{\alpha\beta}^{00}(\omega = 0, \boldsymbol{k} = 0)|_{\pi=0} &= f_{\mathrm{t}}^2 \delta_{\alpha\beta} \\
\chi_{\alpha\beta}^{ij}(\omega = 0, \boldsymbol{k} = 0)|_{\pi=0} &= -f_{\mathrm{s}}^2 \delta^{ij} \delta_{\alpha\beta}. \tag{27}
\end{aligned}$$

Throughout this section, we use an abbreviated notation of $\pi^\alpha = 0$ to denote the ground-state values: $\pi^\alpha = 0$ and the background field A_μ^a and W fixed at physical values given in Eqs. (16). The second and third equations indicate a nonvanishing long-range correlation for the (approximately) conserved currents, which is a manifestation of spontaneous symmetry breaking. Its structure is the same as the familiar symmetry breaking in the Lorentz invariant systems, except for the independent numerical prefactor, which reflects the fact that the propagating speed of magnons is generally not the speed of light. On the other hand, the first equation is peculiar to the nonrelativistic system since the nonvanishing charge density $m \neq 0$ manifestly breaks the Lorentz invariance.

Taking the variation with respect to the background field W, we can also obtain the matching condition for r as

$$r = \left\langle \frac{\delta \mathcal{S}_{\mathrm{eff}}}{\delta W^{33}} \right\rangle\bigg|_{\pi=0}, \tag{28}$$

which is proportional to $\langle \hat{s}_3^n \hat{s}_3^n \rangle$ in the lattice model description. Equations (27) and (28) provide the matching conditions for low-energy coefficients m, f_{t}, f_{s}, and r.

Depending on which coefficients are present, we can classify various magnets into three types: antiferromagnets, ferromagnets, and ferrimagnets. For simplicity, let us consider the simple situation with vanishing explicit symmetry-breaking terms—the background magnetic field B^a, DM interaction D_j^a, and single-ion anisotropy C^{ab}. In this case, we can simplify the quadratic part of the effective Lagrangian as

$$\begin{aligned}
\mathcal{L}_{\mathrm{eff}}^{(2)} &= -\frac{m}{2} \epsilon_{\alpha\beta}^3 \pi^\alpha \partial_0 \pi^\beta \\
&\quad + \frac{f_{\mathrm{t}}^2}{2} \delta_{\alpha\beta} \partial_0 \pi^\alpha \partial_0 \pi^\beta - \frac{f_{\mathrm{s}}^2}{2} \delta_{\alpha\beta} \delta^{ij} \partial_i \pi^\alpha \partial_j \pi^\beta, \tag{29}
\end{aligned}$$

which results in the following equation of motion:

$$\begin{pmatrix} f_{\mathrm{t}}^2 \partial_0^2 - f_{\mathrm{s}}^2 \boldsymbol{\nabla}^2 & m\partial_0 \\ -m\partial_0 & f_{\mathrm{t}}^2 \partial_0^2 - f_{\mathrm{s}}^2 \boldsymbol{\nabla}^2 \end{pmatrix} \begin{pmatrix} \pi^1 \\ \pi^2 \end{pmatrix} = 0. \tag{30}$$

By solving the characteristic equation for the coefficient matrix, we can investigate the number of the independent NG modes and their dispersion relations. The result is summarized as follows:

(i) Antiferromagnet ($f_t \neq 0$, $m = 0$):

$$\text{two NG modes} \quad \text{with} \quad \omega = c_s |\boldsymbol{k}|, \tag{31}$$

(ii) Ferromagnet ($f_t = 0$, $m \neq 0$):

$$\text{one NG mode} \quad \text{with} \quad \omega = \frac{f_s^2}{m} k^2, \tag{32}$$

(iii) Ferrimagnet ($f_t \neq 0$, $m \neq 0$):

one NG mode and one gapped mode

$$\text{with} \quad \omega = \frac{f_s^2}{m} k^2 + O(k^4), \quad \omega = \frac{m}{f_t^2} + O(k^2). \tag{33}$$

We list only positive frequencies here and subsequently, although there are negative frequency solutions with the opposite sign. Here, we have introduced the propagating speed of the antiferromagnetic magnon as $c_s \equiv f_s/f_t$, which is not necessarily the speed of light in contrast to the NG mode in the Lorentz invariant system. Note that the ferro/ferrimagnetic magnons show the quadratic dispersion relation and the number of gapless excitation N_{NG} obeys the general counting rule:

$$N_{NG} = N_{BS} - \text{rank } \rho \quad \text{with} \quad \rho_{ab}(x) \equiv \langle [i\hat{Q}_a, \hat{J}_b^0(x)] \rangle. \tag{34}$$

Here, we introduced the number of the broken symmetry N_{BS} and the so-called Watanabe-Brauner matrix ρ_{ab}, where $\hat{Q}_a = \int d^d x \, \hat{J}_a^0(x)$ ($a = 1, 2, 3$) denotes the Noether charge associated with the SO(3) symmetry. One finds that the counting rule Eq. (34) is completely consistent with the present setup by recalling $N_{BS} = \dim \text{SO}(3)/\text{SO}(2) = 2$ and rank $\rho = 1$ for the collinear ferro/ferrimagnetic ground state or rank $\rho = 0$ for the antiferromagnetic one. Here, we used the fact that our matching condition $\rho_{12}(x) = \langle \hat{J}_3^0(x) \rangle = m$ does not vanish in ferro/ferrimagnets while it does in antiferromagnets. The dispersion relation at small $\boldsymbol{k}$ in the ferrimagnet case given in Eq. (33) reduces to that in the ferromagnet case as $f_t \to 0$ while it does not reduce to that of antiferromagnet in the limit of $m \to 0$. This apparent inconsistency comes from our limiting procedure: we first take the small $\boldsymbol{k}$ limit in Eq. (33) and consider the $m \to 0$ limit. The full dispersion relation for ferrimagnets is available from Eq. (30), which, of course, reproduces that of antiferromagnets when we take $m \to 0$.

IV. LOW-ENERGY SPECTRUM ON HELICAL/SPIRAL PHASE

In this section, we apply the effective Lagrangian Eq. (17) to study low-energy excitation spectra of noncollinear (inhomogeneous) ground states induced by the DM interaction. When the DM interaction is sufficiently large, noncollinear states tend to become the ground state. The simplest of such noncollinear ground states develop a one-dimensional modulation of the spin vector. Depending on the types of the DM interaction, they are called the helical ground state or spiral ground state. Both of them support a gapless NG mode as a low-energy excitation, that is, the phonon associated with the spontaneous breaking of the translation symmetry. Nonetheless, we demonstrate that the form of the dispersion relation is qualitatively different between helical and spiral states.

A. Isotropic dispersion relation in helical ground state

As the first application, we consider the case where the simple combination of the uniaxial DM interaction and easy-axis anisotropic potential along the same direction are present. For simplicity, we choose the following background values for the external fields in the effective Lagrangian Eq. (17):

$$A_0^a = 0, \quad A_i^a = \kappa_i \delta_3^a, \quad \text{and} \quad rW^{ab} = \frac{W}{2} \delta_3^a \delta_3^b. \tag{35}$$

Using this setup, we will show that the system develops helical order in the case of the easy-plane potential ($W < 0$) [55]. Due to the spontaneous breaking of the translational symmetry, the helical ground state is shown to support a translational gapless phonon (NG mode) in the low-energy spectrum irrespective of the types of chiral magnets.

In contrast to the analysis in Sec. III B, we have a noncollinear ground state, which forces us to abandon the description in Eq. (20) in terms of NG bosons on the collinear ground state. We thus here start with the original O(3) nonlinear sigma model description given in Eq. (17). Substituting Eq. (35) into the effective Lagrangian Eq. (17), we obtain

$$\mathcal{L}_{\text{eff}} = \frac{m(n^2 \partial_0 n^1 - n^1 \partial_0 n^2)}{1 + n^3} + \frac{f_t^2}{2} (\partial_0 n^a)^2$$
$$- \frac{f_s^2}{2} (\partial_i n^a - \kappa_i \epsilon_{b3}^a n^b)^2 + \frac{W}{2} (n^3)^2. \tag{36}$$

One should note that the potential $V(n^3) = -W(n^3)^2/2$ favors $n^3 = \pm 1$ (easy axis) if $W > 0$, whereas it favors $n^3 = 0$ (easy-plane) if $W < 0$. To find the ground state, we use the Hamiltonian defined by the Legendre transformation of Eq. (36) as

$$\mathcal{H} = \Pi_a \partial_0 n^a - \mathcal{L}_{\text{eff}}$$
$$= \frac{1}{2f_t^2} \left(\Pi_a - \frac{m(n^2 \delta_a^1 - n^1 \delta_a^2)}{1 + n^3} \right)^2$$
$$+ \frac{f_s^2}{2} (\partial_i n^a - \kappa_i \epsilon_{b3}^a n^b)^2 - \frac{W}{2} (n^3)^2, \tag{37}$$

where we defined the conjugate momentum Π_a as

$$\Pi_a \equiv \frac{\partial \mathcal{L}_{\text{eff}}}{\partial (\partial_0 n^a)} = \frac{m(n^2 \delta_a^1 - n^1 \delta_a^2)}{1 + n^3} + f_t^2 \partial_0 n_a. \tag{38}$$

Noting that the Hamiltonian Eq. (37) is expressed as a sum of the quadratic terms, we try to find a candidate ground-state solution by requiring the first two terms to vanish:

$$\partial_0 n^a = 0, \quad \partial_i n^a - \kappa_i \epsilon_{b3}^a n^b = 0. \tag{39}$$

The solutions of this set of equations are given by

$$\bar{n}^a = \begin{pmatrix} \sqrt{1 - \bar{A}^2} \cos(\boldsymbol{\kappa} \cdot \boldsymbol{x} + \bar{\phi}) \\ -\sqrt{1 - \bar{A}^2} \sin(\boldsymbol{\kappa} \cdot \boldsymbol{x} + \bar{\phi}) \\ \bar{A} \end{pmatrix}, \tag{40}$$

where two real parameters $\bar{A} \in [-1, 1]$ and $\bar{\phi} \in [0, 2\pi)$ denote integration constants, which characterize an orbit on the unit sphere at a constant latitude $n^3 = \bar{A}$. Since we can regard the potential to be a function of these orbits ($n_3 = \bar{A}$), we can find the ground state by just finding the orbit corresponding to
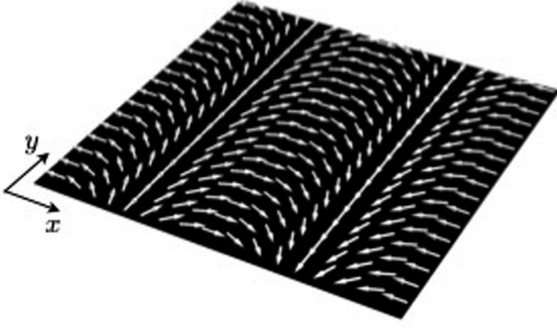
FIG. 2. A schematic picture of the helical ground state in the DM dominant $(2 + 1)$-dimensional magnet.

the minimum of the potential. Thus, we find the ground states as

$$
\bar{A} =
\begin{cases}
\pm 1 & \text{for} \quad W > 0 \\
0 & \text{for} \quad W < 0 \\
\text{arbitrary} \in [-1, 1] & \text{for} \quad W = 0.
\end{cases}
\tag{41}
$$

While the ground state is collinear for $\bar{A} = \pm 1$, it realizes the noncollinear helical order for $|\bar{A}| < 1$. Figure 2 shows a schematic picture of the helical ground-state configuration of n^a with $\bar{A} = 0$ (the orbit circling at the equator). Thus, we find that the helical order is realized along the direction of the DM interaction $\boldsymbol{\kappa}$ when $W \leqslant 0$ (see also Ref. [55]). The fine-tuned case with $W = 0$ is unique in the sense that circles at any latitude give the degenerate classical ground states corresponding to the Kaplan-Shekhtman-Aharony-Entin-Wohlman limit [74,75]. In this case of $W = 0$, BPS soliton solutions in $(1 + 1)$-dimension have been exhaustively worked out in Ref. [55]. One should note that our parametrization of the $(n^3)^2$ term in the potential differs from many previous works, including Ref. [55], where the additional term was present in the potential as $V(n^3) = (-W + \kappa^2)(n^3)^2/2$.

Let us then consider the case with $W < 0$, and investigate the low-energy spectrum on the helical ground state. For that purpose, we consider fluctuations of δA and $\delta \phi$ around the fixed background values $\bar{A} = 0$ and $\bar{\phi} = 0$, and rewrite the effective Lagrangian by promoting $\delta A(x)$ and $\delta \phi(x)$ to dynamical fields. In short, we parametrize the spin vector n^a as

$$
\boldsymbol{n}(x) =
\begin{pmatrix}
\sqrt{1 - (\delta A(x))^2} \cos(\boldsymbol{\kappa} \cdot \boldsymbol{x} + \delta \phi(x)) \\
-\sqrt{1 - (\delta A(x))^2} \sin(\boldsymbol{\kappa} \cdot \boldsymbol{x} + \delta \phi(x)) \\
\delta A(x)
\end{pmatrix}
$$
$$
\simeq
\begin{pmatrix}
\cos(\boldsymbol{\kappa} \cdot \boldsymbol{x} + \delta \phi(x)) \\
-\sin(\boldsymbol{\kappa} \cdot \boldsymbol{x} + \delta \phi(x)) \\
\delta A(x)
\end{pmatrix},
\tag{42}
$$

where, in the second equality, we have retained the leading order of the expansion with respect to the fluctuation (δA and $\delta \phi$) to investigate the low-energy spectra of δA and $\delta \phi$. Substituting this parametrization into the original effective Lagrangian Eq. (36), we now obtain the quadratic part of the Lagrangian for the amplitude mode δA and phase mode $\delta \phi$ as

$$
\mathcal{L}_{\text{eff}}^{(2)} = m(1 - \delta A) \partial_0 \delta \phi + \frac{f_t^2}{2} [(\partial_0 \delta A)^2 + (\partial_0 \delta \phi)^2]
$$
$$
- \frac{f_s^2}{2} [(\partial_i \delta A)^2 + (\partial_i \delta \phi)^2] + \frac{W}{2} (\delta A)^2,
\tag{43}
$$

from which we can read off the following linearized equations of motion:

$$
\begin{pmatrix}
f_t^2 \partial_0^2 - f_s^2 \nabla^2 & -m \partial_0 \\
m \partial_0 & f_t^2 \partial_0^2 - f_s^2 \nabla^2 - W
\end{pmatrix}
\begin{pmatrix}
\delta \phi \\
\delta A
\end{pmatrix}
= 0.
\tag{44}
$$

Note that the equations of motion for the amplitude and phase fluctuations are coupled in the presence of the magnetization parameter m while they decouple for vanishing m. Solving the characteristic equation for the matrix and noting $W = -|W|$, we obtain the dispersion relation in each case of magnets as

(i) Antiferromagnet ($f_t \neq 0$, $m = 0$):

$$
\omega = \frac{f_s}{f_t} |\boldsymbol{k}|, \quad \frac{\sqrt{|W| + (f_s \boldsymbol{k})^2}}{f_t},
\tag{45}
$$

(ii) Ferromagnet ($f_t = 0$, $m \neq 0$):

$$
\omega = \frac{f_s |\boldsymbol{k}| \sqrt{|W| + (f_s \boldsymbol{k})^2}}{m} = \frac{f_s \sqrt{|W|}}{m} |\boldsymbol{k}| + O(|\boldsymbol{k}|^3),
\tag{46}
$$

(iii) Ferrimagnet ($f_t \neq 0$, $m \neq 0$):

$$
\omega = \left(\frac{|W|}{m^2 + |W|} \right)^{\frac{1}{2}} \frac{f_s}{f_t} |\boldsymbol{k}|
$$
$$
+ \frac{m^4}{2\sqrt{|W|}(m^2 + |W|)^5} \frac{(f_s |\boldsymbol{k}|)^3}{f_t} + O(|\boldsymbol{k}|^5),
$$
$$
\omega = \frac{\sqrt{m^2 + |W|}}{f_t} + \frac{2m^2 + |W|}{2(m^2 + |W|)^{3/2}} \frac{f_s^2 \boldsymbol{k}^2}{f_t} + O(\boldsymbol{k}^4).
\tag{47}
$$

We now see that the helical ground state with $W < 0$ supports only one gapless excitation (NG mode, and its dispersion relation is linear with respect to the momentum in all cases. This is in sharp contrast to the limiting case of $W = 0$ in Eq. (47), in which the ferromagnet supports the magnon with a quadratic dispersion.

In the current case ($W < 0$), the dispersion relation at small $\boldsymbol{k}$ in the ferrimagnet case Eq. (47) reduces to that in the antiferromagnet case Eq. (45) in the limit of $m \to 0$ but does not reduce to that in the ferromagnet case of Eq. (46) in the limit of $f_t \to 0$. On the other hand, the dispersion relations for the antiferromagnet in Eq. (45) and ferromagnet in Eq. (46) reduce in the limit $W \to 0$ to Eqs. (31) and (32) for the antiferromagnet and ferromagnet. However, the dispersion relation of the gapless mode of the ferrimagnet in Eq. (47) is singular as $W \to 0$ and does not agree with Eq. (33). This discontinuity is due to the change of the small $\boldsymbol{k}$ behavior from $|W||\boldsymbol{k}|$ at $W < 0$ to $\boldsymbol{k}^2$ at $W = 0$, which is similar to magnon dispersion relations in the collinear ordered phase. Again, the full dispersion relation for ferrimagnets before small-$\boldsymbol{k}$ expansion, which is available from solving Eq. (44), reproduces both ferromagnetic and antiferromagnetic limits.

Let us clarify the symmetry-breaking pattern for the helical ground state. Originally, the effective Lagrangian Eq. (36) enjoys $SO(2)_z$ spin rotation symmetry and spatial translation symmetry $\mathbb{R}^d$. The helical ground state clearly breaks one spatial translation symmetry down to $\mathbb{R}_\perp^{d-1}$ and, thus, one may regard the resulting gapless mode as the translational phonon. However, we note that it is also possible to interpret this gapless mode as the magnon in a rotating frame. This is

because one can also regard the symmetry breaking pattern as

$$SO(2)_z \times \mathbb{R}^d \to \mathbb{R}_{s+\|} \times \mathbb{R}_{\perp}^{d-1}, \quad (48)$$

since the helical ground-state configuration remains invariant under a particular combination of the $SO(2)_z$ spin rotation and spatial translation $\mathbb{R}_\|$ along the modulation, which we expressed as $\mathbb{R}_{s+\|}$. In fact, we can eliminate the DM interaction by performing the field redefinition of the spin vector (see e.g., Ref. [55]) and, as a result, the newly defined spin develops the collinear order so one obtains the corresponding magnon mode. In this interpretation, the linear dispersion with $W < 0$ corresponds to the magnon in the presence of the easy-plane potential, where the remaining $SO(2)_z$ symmetry is spontaneously broken (the spectrum with $W = 0$ corresponds to the magnon without $SO(3)$ symmetry breaking perturbations). In short, one can call the gapless mode in the helical phase the translational phonon or $SO(2)_z$ magnon in the rotating frame.

B. Anisotropic dispersion relation in spiral ground state

Let us next consider $(2 + 1)$-dimensional chiral magnets containing an isotropic (in the x, y plane) DM interaction $D_i^a \propto \delta_i^a$, $i = 1, 2$, which allows a spiral ground state when the DM interaction is more dominant than the potential. To

obtain the simplest explicit solution, we consider the case without a potential (after the DM interactions are explicitly separated from covariant derivatives). Hence our effective Lagrangian is given by

$$\mathcal{L}_{\text{eff}} = \frac{m(n^2 \partial_0 n^1 - n^1 \partial_0 n^2)}{1 + n^3} + \frac{f_t^2}{2}(\partial_0 n^a)^2 - \frac{f_s^2}{2}(\partial_i n^a)^2$$
$$+ f_s^2 \kappa [n^3(\partial_y n^1 - \partial_x n^2) + (n^2 \partial_x - n^1 \partial_y)n^3]. \quad (49)$$

This Lagrangian corresponds to the following choice of background fields with a constant term $-\kappa^2/2$ discarded:

$$A_0^a = 0, \quad A_i^a = -\kappa \delta_i^a, \quad rW_{ab}n^a n^b = -f_s^2 \kappa^2 (n^3)^2. \quad (50)$$

Instead of treating the constrained variable n^a, we now explicitly solve the constraint $n^a n_a = 1$ by using the spherical parametrization of the spin vector $\boldsymbol{n}$ given by

$$\boldsymbol{n} = \begin{pmatrix} \sin\theta\cos\phi \\ \sin\theta\sin\phi \\ \cos\theta \end{pmatrix} \quad \text{with} \quad 0 \leqslant \theta < \pi, \quad 0 \leqslant \phi < 2\pi. \quad (51)$$

Substituting this into Eq. (49), we obtain the Lagrangian in terms of the unconstrained variables:

$$\mathcal{L}_{\text{eff}} = 2m\sin^2\frac{\theta}{2}\partial_0\phi + \frac{f_t^2}{2}[(\partial_0\theta)^2 + \sin^2\theta(\partial_0\phi)^2] - \frac{f_s^2}{2}[(\partial_i\theta)^2 + \sin^2\theta(\partial_i\phi)^2]$$
$$+ f_s^2 \kappa\left[(\cos\phi\partial_y - \sin\phi\partial_x)\theta - \frac{1}{2}\sin 2\theta(\cos\phi\partial_x + \sin\phi\partial_y)\phi\right]. \quad (52)$$

To find a one-dimensionally noncollinear solution, let us assume that the configuration is independent of time t and spatial coordinate y. This assumption is consistent with the equation of motion, thanks to the space-time translational symmetry. Retaining only the x dependence, we find energy density $\mathcal{E}$ of such a configuration as

$$\mathcal{E}[\theta, \phi] = \frac{f_s^2}{2}\left[\left(\frac{d\theta}{dx}\right)^2 + \sin^2\theta\left(\frac{d\phi}{dx}\right)^2\right]$$
$$- f_s^2 \kappa\left[-\sin\phi\frac{d\theta}{dx} - \frac{1}{2}\sin 2\theta\cos\phi\frac{d\phi}{dx}\right]. \quad (53)$$

The equation of motion for ϕ can be solved trivially by taking

$$\phi = \pm\frac{\pi}{2} + 2n\pi, \quad n \in \mathbb{Z}. \quad (54)$$

With this choice, the energy density becomes

$$\mathcal{E}[\theta] = \frac{f_s^2}{2}\left(\frac{d\theta}{dx}\right)^2 \pm f_s^2\kappa\frac{d\theta}{dx}, \quad (55)$$

where the $\pm$ sign corresponds to $\phi = \pm\pi/2 + 2n\pi$. It is interesting to observe that the DM interaction for the one-dimensionally noncollinear configuration becomes a total derivative and does not affect the equation of motion for θ, which becomes

$$\frac{d^2\bar{\theta}(x)}{dx^2} = 0, \quad (56)$$

yielding the following solution:

$$\bar{\theta}(x) = cx + d \quad \text{with} \quad c, d \in \mathbb{R}, \quad (57)$$

where c and d are integration constants. Although all these solutions with arbitrary values of c, d are solutions of the field equations, they can give different energy densities because of the total derivative term induced by the DM interaction. We can minimize the energy density of these solutions,

$$\mathcal{E}[\bar{\theta}] = f_s^2\left(\frac{c^2}{2} \pm \kappa c\right), \quad (58)$$

to find the ground state at the value of $c = \mp\kappa$. Since both signs give physically equivalent ground states, we find the spiral ground state with a moduli parameter d as

$$\bar{\phi} = \frac{\pi}{2}, \quad \bar{\theta}(x) = -\kappa x + d, \quad \text{with} \quad d \in \mathbb{R}. \quad (59)$$

Since this ground-state solution represents the one-dimensional spiral modulation of the spin vector, it is called the spiral phase (see Fig. 3). The most general spiral solution can be obtained by applying simultaneous rotation in the x-y plane and spin vector in the n^1-n^2 plane. The spiral state is similar to the helical state in that both describe the one-dimensional modulations. Nevertheless, the behavior of the collective excitation, or the translational phonon, is qualitatively different, as will be shown below. As a representative spiral state, we take the solution in Eq. (59) as the background to study the dispersion relation of low-energy excitations.
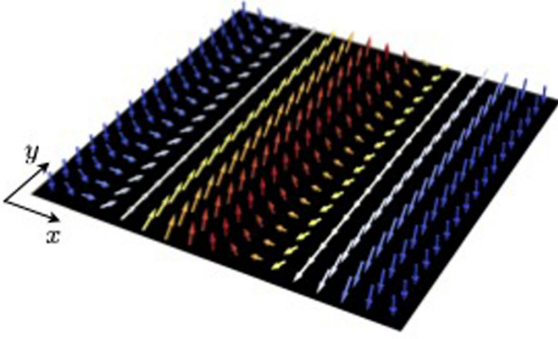
FIG. 3. A schematic picture of the spiral ground state in the $(2 + 1)$-dimensional magnet.

To investigate the low-energy excitation in the spiral ground state, we introduce the fluctuations $\delta\theta$ and $\delta\phi$ around the spiral ground state as

$$\theta(t, \mathbf{x}) = -\kappa x + \delta\theta(t, \mathbf{x}), \quad \phi(t, \mathbf{x}) = \frac{\pi}{2} + \delta\phi(t, \mathbf{x}). \quad (60)$$

Note that the fluctuation field $\delta\theta(t, \mathbf{x})$ appears in the specific combination with the position coordinate $-\kappa x + +\delta\theta(t, \mathbf{x})$ due to the spatial translational symmetry breaking in the spiral phase. This implies that $\delta\theta(t, \mathbf{x})$ is identified as the translational phonon field attached to the translational symmetry breaking.

Then, we substitute this parametrization to the effective Lagrangian Eq. (52) and collect the terms within the quadratic order of fluctuations. We find that it is useful to use $\delta\Omega(x) \equiv \sin(-\kappa x)\delta\phi$ instead of $\delta\phi(x)$. The resulting effective Lagrangian for the fluctuations $\delta\theta$ and $\delta\Omega$ is given by

$$\mathcal{L}_{\mathrm{eff}}^{(2)} = \frac{f_{\mathrm{t}}^2}{2}[(\partial_0\delta\theta)^2 + (\partial_0\delta\Omega)^2] - \frac{f_{\mathrm{s}}^2}{2}[(\partial_i\delta\theta)^2 + (\partial_i\delta\Omega)^2]$$
$$- \frac{f_{\mathrm{s}}^2\kappa^2}{2}(\delta\Omega)^2 + m\delta\theta\partial_0\delta\Omega - 2f_{\mathrm{s}}^2\kappa\sin\kappa x\,\delta\theta\partial_y\delta\Omega. \quad (61)$$

This result shows that the fluctuations $\delta\theta$ and $\delta\Omega$ couple through the first-order time derivative term, and the sinusoidal modulation proportional to the magnitude of the DM interaction κ with the momentum ∂_y perpendicular to the modulation.

Due to the explicit presence of the sinusoidal function, the linear mode analysis will be a little complicated in the same way as the band theory with a periodic potential.

Let us investigate the low-energy spectrum described by Eq. (61). First, we derive the equation of motion given by

$$\left(f_{\mathrm{t}}^2\partial_0^2 - f_{\mathrm{s}}^2\boldsymbol{\nabla}^2\right)\delta\theta - \left(m\partial_0 - 2f_{\mathrm{s}}^2\kappa\sin\kappa x\partial_y\right)\delta\Omega = 0,$$

$$\left(f_{\mathrm{t}}^2\partial_0^2 - f_{\mathrm{s}}^2\boldsymbol{\nabla}^2 + f_{\mathrm{s}}^2\kappa^2\right)\delta\Omega + \left(m\partial_0 - 2f_{\mathrm{s}}^2\kappa\sin\kappa x\partial_y\right)\delta\theta = 0. \quad (62)$$

Performing the Fourier transformation with respect to the time argument, we can rewrite these equations in a matrix form,

$$A(\omega)\vec{\varphi} = H(x)\vec{\varphi} \quad \text{with} \quad \vec{\varphi} \equiv \begin{pmatrix} \delta\theta \\ \delta\Omega \end{pmatrix}, \quad (63)$$

where we introduced the coefficient matrices as

$$A(\omega) \equiv \begin{pmatrix} f_{\mathrm{t}}^2\omega^2 & -im\omega \\ im\omega & f_{\mathrm{t}}^2\omega^2 \end{pmatrix},$$

$$H(x) \equiv f_{\mathrm{s}}^2 \begin{pmatrix} -\boldsymbol{\nabla}^2 & 2\kappa\sin\kappa x\partial_y \\ -2\kappa\sin\kappa x\partial_y & -\boldsymbol{\nabla}^2 + \kappa^2 \end{pmatrix}. \quad (64)$$

Let us first derive the eigenvalue spectra of the reduced Hamiltonian $H(x)$, which are periodic along the x direction as $x \to x + a$ with the period $a \equiv 2\pi/\kappa$. Thanks to the periodicity, we can apply Bloch's theorem [76] by introducing $\vec{\varphi}_k$ as a simultaneous eigenstate for H and the discrete translation $T_a = e^{a\partial_x}$ as

$$H(x)\vec{\varphi}_{k_x}(x) = E_{k_x}\vec{\varphi}_{k_x}(x) \quad \text{and} \quad T_a\vec{\varphi}_{k_x}(x) = e^{ik_xa}\vec{\varphi}_{k_x}(x). \quad (65)$$

Here, the discrete translation operator induces $T_aH(x + a)T_a^{-1} = H(x)$ and $T_a\vec{\varphi}(x) = \vec{\varphi}(x + a)$. Bloch's theorem tells us that we can decompose such an eigenvector as

$$\vec{\varphi}_{k_x}(x) = \int \frac{dk_\perp}{2\pi} \sum_n e^{i(k_x+\kappa n)x + ik_\perp y}\vec{v}_n(\mathbf{k}), \quad (66)$$

with $\vec{v}_n(\mathbf{k}) \equiv (v_n^{(0)}(\mathbf{k}), v_n^{(1)}(\mathbf{k}))^t$. We also have introduced the momentum perpendicular to the modulation direction as $k_\perp$. Note that the momentum along the modulation direction k_x takes a value within the first Brillouin zone: $k_x \in [-\pi/a, \pi/a) = [-\kappa/2, \kappa/2)$. Substituting this vector into the eigenvalue problem, we obtain recurrence relations among v_n as

$$f_{\mathrm{s}}^2\left([(k_x + \kappa n)^2 + k_\perp^2]v_n^{(0)}(\mathbf{k}) + \kappa k_\perp[v_{n-1}^{(1)}(\mathbf{k}) - v_{n+1}^{(1)}(\mathbf{k})]\right) = E_n(\mathbf{k})v_n^{(0)}(\mathbf{k}),$$

$$f_{\mathrm{s}}^2\left(-\kappa k_\perp[v_{n-1}^{(0)}(\mathbf{k}) - v_{n+1}^{(0)}(\mathbf{k})] + [(k_x + \kappa n)^2 + k_\perp^2 + \kappa^2]v_n^{(1)}(\mathbf{k})\right) = E_n(\mathbf{k})v_n^{(1)}(\mathbf{k}). \quad (67)$$

As expected, the nondiagonal element is proportional to $\kappa k_\perp$. Thus, we can derive the exact result for the eigenvalue with the eigenfunction on the momentum plane $k_\perp = 0$ as

$$E_n^{(0)}(k_x, 0) = f_{\mathrm{s}}^2(k_x + \kappa n)^2,$$

$$E_n^{(1)}(k_x, 0) = f_{\mathrm{s}}^2[(k_x + \kappa n)^2 + \kappa^2]. \quad (68)$$

It is clear that the former branch of the solution with $n = 0$ gives the lowest-lying eigenvalue, and all the bands with

$n \neq 0$ have gaps determined by the magnitude of the DM interaction κ.

Apart from the $k_\perp = 0$ plane, we need to solve the coupled infinite-dimensional recurrence relation. We observe that the coupling between neighboring bands n and $n + 1$ is proportional to $\kappa k_\perp$ and that the recurrence relations separate into two sets: those relating $v_{2n}^{(0)}$ with $v_{2n+1}^{(1)}$ and those relating $v_{2n}^{(1)}$ with $v_{2n+1}^{(0)}$. These facts allow us to use an approximation to take account of only $2n + 1$ bands between the

$-n$th and nth bands to obtain eigenvalues of the Hamiltonian at small $\boldsymbol{k}^2/\kappa^2$ for low-lying states. Defining $\omega_n^+ \equiv (k_x + n\kappa)^2 + k_\perp^2 + \kappa^2$ and $\omega_n^- \equiv (k_x + n\kappa)^2 + k_\perp^2$, we find an explicit form of the eigenvalue problem in the three-band truncated approximation as the following two sets of 3×3 matrix equations:

$$\begin{pmatrix} \omega_1^+ - \frac{E(\boldsymbol{k})}{f_s^2} & -\kappa k_\perp & 0 \\ -\kappa k_\perp & \omega_0^- - \frac{E(\boldsymbol{k})}{f_s^2} & \kappa k_\perp \\ 0 & \kappa k_\perp & \omega_{-1}^+ - \frac{E(\boldsymbol{k})}{f_s^2} \end{pmatrix} \begin{pmatrix} v_1^{(1)}(\boldsymbol{k}) \\ v_0^{(0)}(\boldsymbol{k}) \\ v_{-1}^{(1)}(\boldsymbol{k}) \end{pmatrix} = 0, \tag{69}$$

$$\begin{pmatrix} \omega_1^- - \frac{E(\boldsymbol{k})}{f_s^2} & \kappa k_\perp & 0 \\ \kappa k_\perp & \omega_0^+ - \frac{E(\boldsymbol{k})}{f_s^2} & -\kappa k_\perp \\ 0 & -\kappa k_\perp & \omega_{-1}^- - \frac{E(\boldsymbol{k})}{f_s^2} \end{pmatrix} \begin{pmatrix} v_1^{(0)}(\boldsymbol{k}) \\ v_0^{(1)}(\boldsymbol{k}) \\ v_{-1}^{(0)}(\boldsymbol{k}) \end{pmatrix} = 0. \tag{70}$$

We find discrete energy bands $E_n(\boldsymbol{k})$ labeled by $n = 0, 1, 2, \cdots$, as a function of momentum $\boldsymbol{k}$ in the first Brillouin zone, by solving the third-order equations for vanishing determinant of the three-band equations. Similarly, we can also consider the five-band truncated approximation. The ground state eigenvalue in the five-band approximation is obtained by solving the following 5×5 matrix equations:

$$\begin{pmatrix} \omega_2^+ - \frac{E(\boldsymbol{k})}{f_s^2} & -\kappa k_\perp & 0 & 0 & 0 \\ \kappa k_\perp & \omega_1^+ - \frac{E(\boldsymbol{k})}{f_s^2} & -\kappa k_\perp & 0 & 0 \\ 0 & -\kappa k_\perp & \omega_0^- - \frac{E(\boldsymbol{k})}{f_s^2} & \kappa k_\perp & 0 \\ 0 & 0 & \kappa k_\perp & \omega_{-1}^+ - \frac{E(\boldsymbol{k})}{f_s^2} & -\kappa k_\perp \\ 0 & 0 & 0 & \kappa k_\perp & \omega_{-2}^+ - \frac{E(\boldsymbol{k})}{f_s^2} \end{pmatrix} \begin{pmatrix} v_2^{(0)}(\boldsymbol{k}) \\ v_1^{(1)}(\boldsymbol{k}) \\ v_0^{(0)}(\boldsymbol{k}) \\ v_{-1}^{(1)}(\boldsymbol{k}) \\ v_{-2}^{(0)}(\boldsymbol{k}) \end{pmatrix} = 0. \tag{71}$$

Figure 4 shows the comparison of the eigenvalues $E_n(0, k_\perp)$ with the three-band and five-band approximations. Note that while the results for the three-band approximation (dashed lines) and five-band approximation (solid lines) are not so different at the low-$k_\perp$ region and the low-lying band, the deviation appears at high-$k_\perp$ regions and at higher bands. As we increase the number of bands in the approximation, we, of course, obtain more bands of eigenvalues. We are interested in the dispersion relation at small values of momentum, especially for low-lying states. Because the coupling between neighboring bands is proportional to $k_\perp/\kappa$, we can use an expansion in powers of $k_\perp/\kappa$ to evaluate energy eigenvalues. We find that the $(2n + 1)$-band approximation gives an exact result for the lowest-band spectrum $E_0(\boldsymbol{k})/(f_s^2\kappa^2)$ up to terms of order $(k_\perp/\kappa)^{2n}$ in powers of $(k_\perp/\kappa)^2$.

Once eigenvalues of the reduced Hamiltonian H are given in terms of the band energy spectra $E_n(\boldsymbol{k})$ in the momentum space with the corresponding eigenvector $\vec{\varphi}_n$, we can obtain the dispersion relation by solving the following equation [recall Eqs. (63) and (64)]:

$$\begin{pmatrix} f_t^2\omega^2 - E_n(\boldsymbol{k}) & -im\omega \\ im\omega & f_t^2\omega^2 - E_n(\boldsymbol{k}) \end{pmatrix} \vec{\varphi}_n = 0. \tag{72}$$

To find nontrivial eigenvectors, we require the determinant of the coefficient matrix to vanish. This characteristic equation gives the dispersion relations given by

(i) Antiferromagnet ($f_t \neq 0$, $m = 0$):

$$\omega_n(\boldsymbol{k}) = \frac{\sqrt{E_n(\boldsymbol{k})}}{f_t} = c_s\frac{\sqrt{E_n(\boldsymbol{k})}}{f_s} \quad \text{(two modes)}, \tag{73}$$

(ii) Ferromagnet ($f_t = 0$, $m \neq 0$):

$$\omega_n(\boldsymbol{k}) = \frac{E_n(\boldsymbol{k})}{m} \quad \text{(one mode)}, \tag{74}$$

(iii) Ferrimagnet ($f_t \neq 0$, $m \neq 0$):

$$\omega_n(\boldsymbol{k}) = \frac{\sqrt{m^2 + 4f_t^2 E_n(\boldsymbol{k})} \pm m}{2f_t^2} \quad \text{(two modes)}, \tag{75}$$

where we again introduced $c_s \equiv f_s/f_t$. As is the case for the collinear ground state, the number of independent modes for ferromagnets ($f_t \neq 0$, $m = 0$) is half that of the antiferromagnets ($f_t = 0$, $m \neq 0$) or ferrimagnets ($f_t \neq 0$, $m \neq 0$). This is because the vanishing f_t^2 makes two fluctuation components $\delta\theta$ and $\delta\Omega$ to be one canonically conjugate pair of dynamical variables so they just give one independent degree
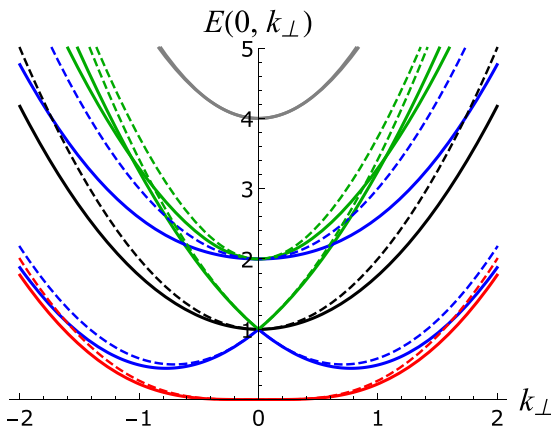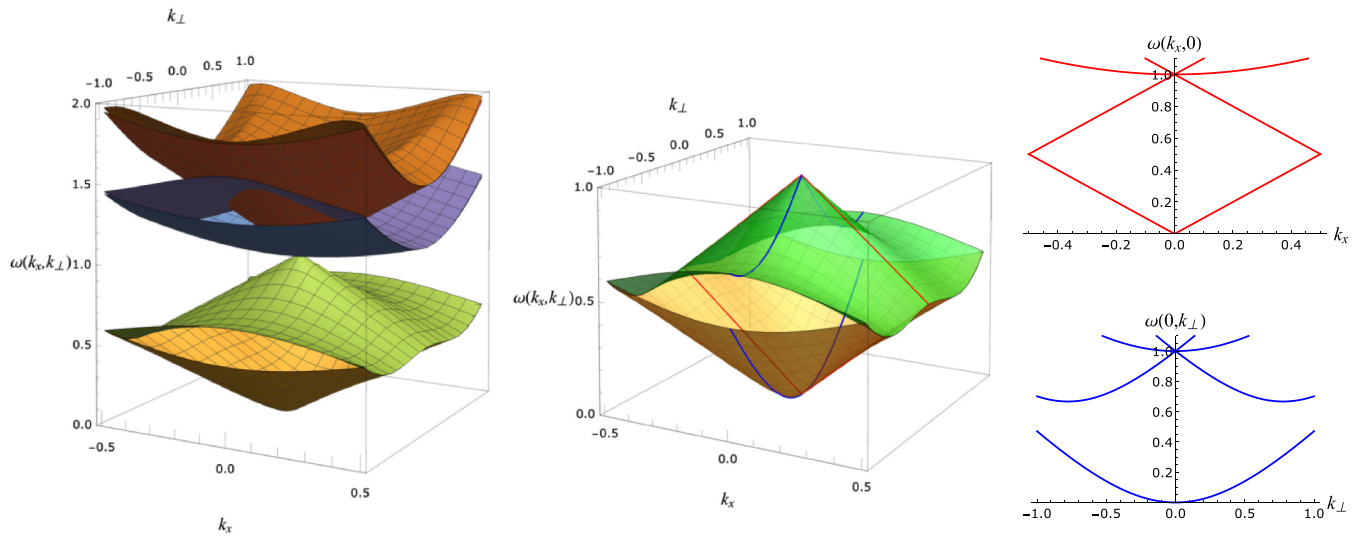

$E(0, k_\perp)$

FIG. 4. A comparison of the eigenvalue $E(0, k_\perp)$ with the three-band approximation (dashed lines) vs five-band approximation (solid lines) on the $k_x = 0$ plane ($\kappa = 1$).

FIG. 5. Low-energy spectrum for the antiferromagnetic spiral phase with the five-band approximation ($\kappa = 1$, $f = 1$).

of freedom in contrast to the case of other magnets, where they become two independent degrees.

Equations (73)–(75) enable us to clarify the low-energy spectrum of the spiral phase from the approximated eigenvalue $E_n(k_x, k_\perp)$. The resulting dispersion relations with the five-band approximation are shown in Figs. 5–8 (note that k_x takes the value in $k_x \in [-\kappa/2, \kappa/2]$ while $k_\perp$ can be any real number $k_\perp \in \mathbb{R}$). One sees that the lowest branch of the bands ($n = 0$) gives the gapless excitation, which dominates the low-energy behavior of the spiral phase. We identify this gapless mode as the NG mode, or the translational phonon, attached to the spatial translatinoal symmetry breaking in the spiral phase. Besides, we also have other bands ($n = \pm 1, \pm 2$ in the current working accuracy) corresponding to the gapped excitation in the first Brillouin zone: $k_x \in [-\kappa/2, \kappa/2]$. Recall that the number of the independent mode is different, as shown in Eqs. (73)–(75): all spectra for the antiferromagnetic case ($f_t \neq 0$, $m = 0$) are doubly degenerated, and the ferrimag-

netic case ($f_t \neq 0$, $m \neq 0$) breaks that degeneracy, so more surfaces can be seen in the leftmost panels of Figs. 7 and 8. We also note that an asymmetry of the spectrum with respect to the momentum inversion induced by the DM interaction is absent in Figs. 7 and 8. This is because our spectrum should be regarded as those for phonons and not for magnons. In other words, the $-\kappa x$ term appearing in Eq. (60) shifts the spectrum of the translational phonon so the momentum asymmetry is hidden in the phonon spectrum.

The rightmost panels in Figs. 5–8 show the section of the low-energy spectrum at $k_x = 0$ and $k_\perp = 0$, respectively. In sharp contrast to the helical phase, the fluctuation spectrum at the low-energy region shows anisotropic behaviors. This peculiar behavior results from the anisotropic behavior of the eigenvalue $E_{n=0}(k_x, k_\perp)$,

$$E_{n=0}(k_x, k_\perp) = k_x^2 - \frac{k_x^2 k_\perp^2}{\kappa^2} + \frac{3k_\perp^4}{8\kappa^2} + \cdots, \qquad (76)$$
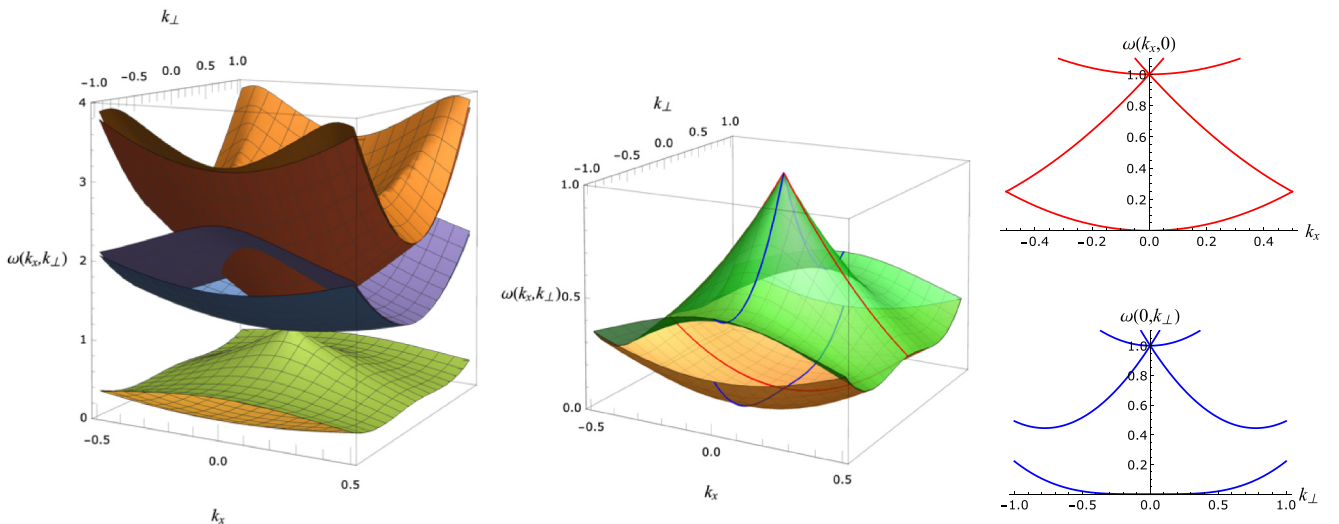
FIG. 6. Low-energy spectrum for the ferromagnetic spiral phase with the five-band approximation ($\kappa = 1$, $m = 1$).
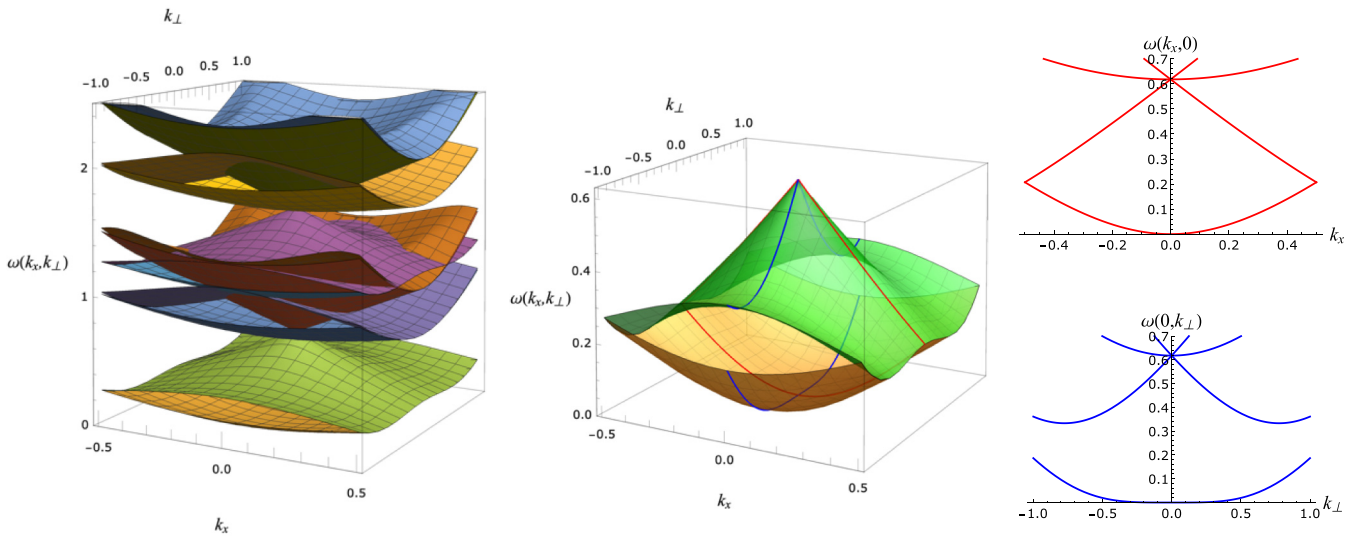
FIG. 7. Low-energy spectrum for the ferrimagnetic spiral phase with the five-band approximation ($\kappa = 1$, $f^2 = 1$, $m = 0.5$).

which is exact up to the order of $k_\perp^4$ in powers of $k_\perp/\kappa$, and can be obtained in the five-band approximation in Eq. (71).

Using Eqs. (73)–(75), we find the low-energy spectrum for the spiral phase. Depending on the type of magnets, we find the dispersion relation for the lowest (gapless) mode as follows:

(i) Antiferromagnet:

$$
\omega_{n=0}(\boldsymbol{k}) = \begin{cases} c_s|k_x|\left(1 - \frac{k_\perp^2}{2\kappa^2} \right. \\ \qquad \left. + \frac{3k_\perp^4}{16\kappa^2|k_x|^2} + \cdots\right) & \text{if } k_x \neq 0, \\ c_s\sqrt{\frac{3}{8}}\frac{k_\perp^2}{\kappa} + \cdots & \text{if } k_x = 0, \end{cases} \quad (77)
$$

(ii) Ferromagnets or ferrimagnets:

$$
\omega_{n=0}(\boldsymbol{k}) = \frac{f_s^2}{m}\left[k_x^2\left(1 - \frac{k_\perp^2}{\kappa^2}\right) + \frac{k_\perp^4}{2\kappa^2} + \cdots\right]. \quad (78)
$$

This gapless excitation is identified as the NG mode associated with the spontaneous symmetry breaking of the one-dimensional translation. The anisotropic dispersion relation is a remarkable property of the one-dimensional modulation consistent with the result from a symmetry-based general approach [32]. We also note that ferrimagnets have another branch of the gapped mode, whose gap is controlled by the magnetization parameter m. Thus, the gapped mode can appear with a relatively small gap when $m/(f_s f_t \kappa) < 1$ (compare Figs. 7 and 8).

The energy spectrum in the spiral phase is qualitatively different from that in the helical phase (even the numbers of the gapless mode in antiferromagnets is different). Moreover, in the spiral phases, the low-momentum behaviors of the energy spectrum are also different between the antiferromangets and ferro/ferrimagnets. We shall explain these results from the symmetry viewpoint. First, the symmetry-breaking
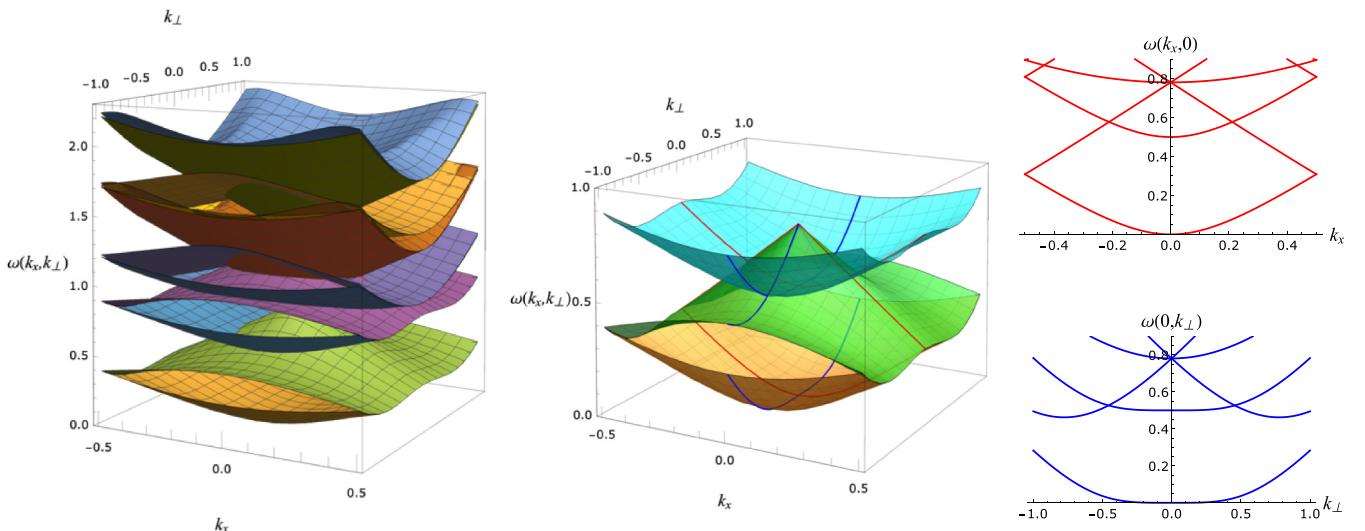

FIG. 8. Low-energy spectrum for the ferrimagnetic spiral phase with the five-band approximation ($\kappa = 1$, $f^2 = 1$, $m = 1$).

pattern is different from the helical phase. In addition to the spatial translation, the effective Lagrangian Eq. (49) remains invariant under a simultaneous rotation in the spin and real spaces (recall that one of the symmetry-breaking terms A_i^a is expressed by the isotropic tensor δ_i^a, which ties the spin and spatial indices). As a result, we identify that the model Eq. (49) originally enjoys $SO(2)_{s+l} \times \mathbb{R}^2$ symmetry, where $SO(2)_{s+l}$ denotes the simultaneous rotation in the spin and real spaces. The spiral ground state then breaks $SO(2)_{s+l}$ symmetry as well as one spatial translation symmetry so the symmetry breaking pattern is identified as

$$SO(2)_{s+l} \times \mathbb{R}^2 \to \mathbb{R}_\perp^1. \tag{79}$$

We clearly see that the number of broken symmetries is different from that in the helical phase [recall Eq. (48)]. The fluctuation fields $\delta\theta$ and $\delta\phi$ correspond to the NG field attached to these broken symmetries. This identification seems to result in the presence of two gapless NG modes in the spiral phase, but we need to be careful whether they describe independent modes or not.

To clarify this point, let us investigate Noether charges based on the original effective Lagrangian Eq. (49). For that purpose, we recall that the $SO(2)_{s+l}$ and $\mathbb{R}_\parallel^1$ (or the broken translational) symmetries with infinitesimal transformation parameters ϵ and ξ act on the field $\boldsymbol{n}$ as

$$\delta n^1 = \epsilon(n^2 + iL_z n^1) + \xi \partial_x n^1$$
$$\delta n^2 = \epsilon(-n^1 + iL_z n^2) + \xi \partial_x n^2$$
$$\delta n^3 = iL_z n^3 + \xi \partial_x n^3, \tag{80}$$

where we defined the orbital angular momentum operator $L_z \equiv -i(y\partial_x - x\partial_y)$. This transformation rule allows us to find the corresponding Noether charge densities as

$$\rho(x) = m\left[1 - n^3 + \frac{n^2 iL_z n^1 - n^1 iL_z n^2}{1 + n^3}\right]$$
$$+ f_t^2[n^2 \partial_0 n^1 - n^1 \partial_0 n^2 + i\delta_{ab}L_z n^a \partial_0 n^b], \tag{81}$$

$$p_x(x) = \frac{m(n^2 \partial_x n^1 - n^1 \partial_x n^2)}{1 + n^3} + f_t^2 \delta_{ab} \partial_0 n^a \partial_x n^b, \tag{82}$$

where we used the normalization condition $\boldsymbol{n}^2 = 1$ to rewrite $\rho(x)$. Then, noting that the conserved charge $Q = \int d^3x \rho(x)$ and $P_x = \int d^2x p_x(x)$ generates the symmetry transformations, we find the ground-state expectation value of the Noether charge's commutator as

$$\langle[iP_x, \rho(x)]\rangle_{gs} = -m\partial_x \bar{n}^3(x) = -m\kappa \sin(-\kappa x + d), \tag{83}$$

which is nonvanishing in the ferro/ferrimagnetic case ($m \neq 0$). Interestingly, the right-hand-side of the commutator Eq. (83) is given by the topological charge density (see, e.g., Ref. [77]).

In summary, we find that the ferro/ferrimagnetic spiral phase supports the nonvanishing ground-state commutator between the Noether charges attached to the broken symmetries. This is a primary reason why two NG fields ($\delta\theta, \delta\phi$) do not describe two independent gapless modes but rather the coupled mode in the ferro/ferrimagnetic spiral phase, whose dispersion relation is further modified from those in antiferromagnets. In other words, we identify that the NG fields $\delta\theta$

and $\delta\phi$ form one type-B NG mode in the ferri/ferromagnetic spiral phase while they give two independent type-A NG modes in the antiferromagnetic one.

A remark on the possible breakdown of the long-range order is in order. Due to its peculiar low-$k_\perp$ behavior of the dispersion relation—quadratic for antiferromagnet and quartic for ferro/ferrimagnets—one may wonder whether it does affect the fate of the spiral phase to be disordered or to be the quasi-long-range order. At zero temperature, we may not encounter an infrared divergence for the correlation function of NG modes thanks to the frequency (and k_x) integral. In particular, the zero-temperature ferro/ferrimagnets are free from such a dangerous fluctuation contribution because one finds no contribution after performing the frequency integral. This situation is similar to the fact that the Mermin-Wagner theorem [78–80] does not apply to the zero-temperature $(1 + 1)$-dimensional ferromagnet. Nevertheless, in finite-temperature systems, all magnets could suffer from the divergent fluctuation contribution, so they may develop the quasi-long-range order (or may be disordered) instead of the true long-range order (see, e.g., Ref. [6]). It is interesting to investigate the fate of the spiral phase at the finite temperature, but it is beyond the scope of this paper.[5]

Before closing this section, we comment on the degenerate point in the spectrum. As we learn at the beginning of the band theory, the band crossing is usually avoided because of the level repulsion, which results from nondiagonal matrix elements of the involved energy states. However, as shown in Figs. 5–8, we find several crossing points at the higher bands. This is because every band in the current model only couples to their nearest-neighboring bands so no level repulsion takes place between non-nearest neighbors. In that sense, most of the degenerate points appear just accidentally. However, there is a special degenerate point $(k_x, k_\perp) = (\pm\kappa/2, 0)$ located at the boundary of the Brillouin zone, where all bands show twofold degeneracy. This twofold degeneracy has a simple origin: First, there is no coupling between different bands when $k_\perp = 0$, so the k_x spectrum on the $k_\perp = 0$ plane is continuous, as given in Eq. (68). Second, the k_x spectrum has to live within the first Brillouin zone because of the periodicity in the x direction. Therefore, the twofold degeneracy at $(k_x, k_\perp) = (\pm\kappa/2, 0)$ is inevitable.

V. MAGNON PRODUCTION BY INHOMOGENEOUS MAGNETIC FIELD

In this section, we consider the production rate of magnons from the collinear (homogeneous) ground state in $(d + 1)$ dimensions caused by an inhomogeneous magnetic field as another application of the EFT of magnons. This mechanism gives a magnon analog of a pair creation of charged particles by an electric field—the Schwinger mechanism [65,66,68]. We show that the magnon production rate (or ground-state decay rate) is controlled by an effective mass of the magnon consisting of the quadratic term of the potential and the ratio of the coefficients of the linear and quadratic time derivative

---

[5]See Ref. [121] for a recent discussion for the fate of the Fulde-Ferrell-Larkin-Ovchinnikov superfluid phase.

terms. Hence, we will find different types of magnets (ferro-
, antiferro-, ferrimagnets) give drastically different magnon
production rates.

A. Setup

Suppose that our spin system possesses a potential with
an easy-axis anisotropy and develops the collinear ground
state. In addition, we apply an inhomogeneous magnetic field
along the spin direction of the ground state and investigate the
resulting dynamics of magnons. We also assume for simplicity
that there is no DM interaction. This situation is described
by the effective Lagrangian with the following background
values of the external fields:

$$A_0^a = \mu B(x)\delta_3^a, \quad A_i^a = 0, \quad \text{and} \quad rW^{ab} = \frac{M^2}{2}\delta_3^a\delta_3^b, \quad (84)$$

with $M^2 > 0$ (easy axis). We also assume the sign of the
background magnetic field as $B(x) \geqslant 0$, so the ground state is
fixed as $\langle \boldsymbol{n} \rangle = (0, 0, 1)^t$. Substituting these background values
into the effective Lagrangian Eq. (20), we obtain the effec-
tive Lagrangian at the quadratic order of fluctuation fields
π^α ($\alpha = 1, 2$) around the ground state $\langle \boldsymbol{n} \rangle = (0, 0, 1)^t$ as

$$\mathcal{L}^{(2)} = -\frac{m}{2}\epsilon_{\alpha\beta}^3\pi^\alpha\partial_0\pi^\beta + \frac{f_t^2}{2}\delta_{\alpha\beta}D_0\pi^\alpha D_0\pi^\beta$$
$$- \frac{f_s^2}{2}\delta^{ij}\delta_{\alpha\beta}\partial_i\pi^\alpha\partial_j\pi^\beta - \frac{m\mu B(x) + M^2}{2}(\pi^\alpha)^2. \quad (85)$$

One sees that the easy-axis potential generates the mass
term proportional to M^2 for the magnon. The effect of
the applied magnetic field appears inside the covariant time
derivative and the mass term if $m \neq 0$. To obtain the pro-
duction rate of magnons due to the inhomogeneous magnetic
field, we only need to consider the above quadratic effective
Lagrangian. Hence, we neglect the interaction term in the
following.

The occurrence of the magnon pair production becomes
clear by mapping our model to the system of a relativistic
charged scalar field. For that purpose, we introduce a new
complex scalar field Φ defined by the linear combination of
magnon fluctuations π^1 and π^2 as

$$\begin{cases} \Phi \equiv \frac{1}{\sqrt{2}}(\pi^1 + i\pi^2) \\ \Phi^* \equiv \frac{1}{\sqrt{2}}(\pi^1 - i\pi^2) \end{cases} \Leftrightarrow \begin{cases} \pi^1 \equiv \frac{1}{\sqrt{2}}(\Phi + \Phi^*), \\ \pi^2 \equiv \frac{1}{\sqrt{2}i}(\Phi - \Phi^*). \end{cases} \quad (86)$$

This transformation enables us to rewrite the effective La-
grangian in terms of the complex scalar field Φ as

$$\mathcal{L}^{(2)} = f_t^2 D_0\Phi^* D_0\Phi - \frac{im}{2}[\Phi D_0\Phi^* - \Phi^* D_0\Phi]$$
$$- f_s^2\delta^{ij}\partial_i\Phi^*\partial_j\Phi - M^2\Phi^*\Phi, \quad (87)$$

where the covariant derivative acting on π^α is translated to
that acting on the complex scalar field:

$$D_0\Phi = \partial_0\Phi + i\mu B\Phi, \quad D_0\Phi^* = \partial_0\Phi^* - i\mu B\Phi^*. \quad (88)$$

Apart from the background scalar potential $A_0(x) = \mu B(x)$,
the effective Lagrangian Eq. (87) takes a familiar form de-
scribing a relativistic charged scalar field except for the linear
time derivative term, which manifestly breaks the Lorentz
symmetry (with an effective speed of light $c_s = f_s/f_t$). The

present model Eq. (87) with a general f_t^2/m interpolates
the relativistic (quadratic time derivative) to a nonrelativis-
tic (linear time derivative) charged scalar field [81]. In fact,
by changing the ratio of the low-energy coefficient f_t^2/m,
we can interpolate two limiting regimes. Let us denote the
characteristic energy scale as k. When $f_t^2/m \gg k$, one can
neglect the second term and the model Eq. (87) reduces to
the usual relativistic charged scalar field. On the other hand,
when $f_t^2/m \ll k$, one can instead throw away the first term
and the model Eq. (87) describes a bosonic Schrödinger field
(see, e.g., Ref. [81] for more detailed discussions).

We observe that this Lorentz-symmetry breaking term can
be regarded as a chemical potential corresponding to the
$U(1) \simeq SO(2)$ symmetry in the relativistic charged scalar
model. Therefore, we can absorb the linear time derivative
term into the temporal component of the external gauge field
by defining a modified covariant derivative $\mathcal{D}_\mu\Phi$ as

$$\mathcal{D}_\mu\Phi \equiv \partial_\mu\Phi - i\mathcal{A}_\mu\Phi, \quad \mathcal{D}_0\Phi^* \equiv \partial_\mu\Phi^* + i\mathcal{A}_\mu\Phi^*, \quad (89)$$

with an inhomogeneous scalar potential :

$$\mathcal{A}_0(x) \equiv \frac{m}{2f_t^2} - \mu B(x), \quad \mathcal{A}_i = 0. \quad (90)$$

We can now rewrite the effective Lagrangian Eq. (87) to a
more useful expression, paying a cost of a constant mass shift,
leading to the following effective action:

$$\mathcal{S}_{\text{eff}}[\Phi; \mathcal{A}_0]$$
$$= \int d^4x \left[f_t^2\mathcal{D}_0\Phi^*\mathcal{D}_0\Phi - f_s^2\delta^{ij}\mathcal{D}_i\Phi\mathcal{D}_j\Phi - M_{\text{eff}}^2\Phi^*\Phi \right], \quad (91)$$

with the effective mass M_{eff} defined by

$$M_{\text{eff}}^2 \equiv M^2 + \frac{m^2}{4f_t^2}. \quad (92)$$

Therefore, our problem is mapped to that of a relativistic
charged scalar field described by the action Eq. (91) with
the effective mass Eq. (92) and the inhomogeneous external
electric potential Eq. (90). Thanks to unbroken $U(1) \simeq SO(2)$
symmetry, one can classify magnon excitations into those
with positively/negatively charged excitations under $U(1) \simeq SO(2)$ symmetry. In fact, $U(1)$ symmetry acts on field vari-
ables Φ and Φ^* as $\Phi \to e^{-i\theta}\Phi$ and $\Phi^* \to e^{i\theta}\Phi^*$. Therefore,
the background magnetic field in $\mathcal{A}_0(x)$ couples to Φ and
Φ^* with opposite charges in a similar manner with the elec-
tron and positron coupled to the electric field in quantum
electrodynamics. Motivated by this observation, we call the
collective excitation described by Φ and Φ^* magnons and
antimagnons. Intuitively speaking, they describe the fluctua-
tions of the spin vector with clockwise and counterclockwise
rotation seen from the north pole.

We here recall that the relativistic charged scalar also
shows the Schwinger mechanism as discussed by Weisskopf
[67] (see, e.g., Ref. [82] for a recent review on the Schwinger
mechanism). Therefore, as a consequence of our mapping to
the effective action Eq. (91), we can carry over all the re-
sults on the Schwinger mechanism for the relativistic charged
scalar by simply replacing the electric field with $E_i \equiv \partial_i\mathcal{A}_0 - \partial_0\mathcal{A}_i = -\mu\partial_i B$ and the mass with M_{eff}^2. To investigate the

magnon production, we consider a simple inhomogeneous magnetic field profile linear in x,

$$B(x) = -b(x - x_{\text{ref}}), \tag{93}$$

with $b > 0$. We assume that $n^3 = +1$ is the collinear ground state. To assure it, we can take a finite interval of x, let x_{ref} to the right of the region, and then take the limit of an infinitely large region ($x_{\text{ref}} \to \infty$). In this limit, we obtain the positive linearly decreasing inhomogeneous magnetic field applied to the $n^3 = +1$ collinear ground state. Similarly to the Schwinger mechanism of charged particle pair production by a constant electric field,[6] we expect to obtain the pair production rate of magnon and antimagnon by this linearly decreasing magnetic field. We will compute this production rate in an idealized situation of an infinite x interval in the following.

B. Magnon production rate

To evaluate the magnon production rate, we use the generating functional in our setup. The generating functional as a functional of the gauge potential $\mathcal{A}$ is given by

$$\begin{aligned} Z[\mathcal{A}] = e^{iW[\mathcal{A}]} &\equiv \lim_{T \to \infty} \langle 0 | e^{-i\hat{H}_\Phi(\mathcal{A})T} | 0 \rangle \\ &= \mathcal{N} \int \mathcal{D}\Phi \, e^{i\mathcal{S}_{\text{eff}}[\Phi; \mathcal{A}]}, \end{aligned} \tag{94}$$

where $|0\rangle$ denotes the collinear vacuum state and $\hat{H}_\Phi(\mathcal{A})$ is the Hamiltonian of the magnon under the inhomogeneous magnetic field obtained from the Lagrangian Eq. (87) ($\mathcal{N}$ is a normalization constant). In the language of the relativistic charged scalar field, we can regard the slope of the magnetic field b as the applied constant electric field because of $E^x = \partial_x \mathcal{A}_0(x) - \partial_0 \mathcal{A}_x = \mu b$. The generating functional (94) defines the vacuum-to-vacuum transition amplitude, and its imaginary part, if present, can be regarded as the ground state decay rate, or the magnon pair production rate. Thus, we will evaluate the imaginary part of the generating functional below.

One nice way to evaluate the generating functional is the world-line formalism, which was originally developed by Feynman [83,84] along the line of the proper-time formalism of Fock and Nambu [85,86] (see, e.g., Refs. [82,87,88] for reviews on the world-line formalism). We use the world-line formalism, which will be briefly described subsequently to make the paper self-contained. Here, we introduce the effective Minkowski metric $\eta_{\mu\nu} = \text{diag}(-f_t^{-2}, f_s^{-2}, \cdots, f_s^{-2})$ and $\eta^{\mu\nu} = \text{diag}(-f_t^2, f_s^2, \cdots, f_s^2)$, which allows us to express the effective action in a covariant manner as

$$\mathcal{S}_{\text{eff}}[\Phi; \mathcal{A}] = \int d^{d+1}x \, \Phi^*[\eta^{\mu\nu}\mathcal{D}_\mu\mathcal{D}_\nu - M_{\text{eff}}^2]\Phi. \tag{95}$$

Then, performing the Gaussian integral and using $\ln \det A = \text{Tr} \ln A$, we can rewrite the generating functional as

$$iW[\mathcal{A}] = -\ln \det\left[-\mathcal{D}^2 + M_{\text{eff}}^2\right] = -\text{Tr} \ln\left[-\mathcal{D}^2 + M_{\text{eff}}^2\right], \tag{96}$$

with $\mathcal{D}^2 = \eta^{\mu\nu}\mathcal{D}_\mu\mathcal{D}_\nu$. We also have introduced the normalization factor by putting the path-integral in the absence of the background field. Since the normalization does not play an essential role in our discussion, we will omit it below. Using a zeta function regularization, we obtain the following identity for an operator O:

$$\ln(O - i\epsilon) = -\int_0^\infty \frac{ds}{s} e^{is(-O+i\epsilon)} \quad \text{with} \quad \epsilon > 0, \tag{97}$$

where s denotes the so-called proper time. With the choice of $O = \frac{1}{2}[-\mathcal{D}^2 + M_{\text{eff}}^2]$, this identity enables us to express the generating functional in terms of the proper time integral as follows:

$$iW[\mathcal{A}] = \int_0^\infty \frac{ds}{s} e^{-\epsilon s} e^{-\frac{i}{2}M_{\text{eff}}^2 s} \text{Tr}(e^{-is\hat{H}(\mathcal{A})}), \tag{98}$$

where we introduced the differential operator $\hat{H}(\mathcal{A})$ by

$$\hat{H}(\mathcal{A}) = \frac{\eta^{\mu\nu}}{2}[\hat{p}_\mu - \mathcal{A}_\mu(\hat{x})][\hat{p}_\nu - \mathcal{A}_\nu(\hat{x})] \quad \text{with} \quad \hat{p}_\mu \equiv -i\partial_\mu. \tag{99}$$

One can see that this differential operator is nothing but the Hamiltonian for one-particle quantum mechanics, where the associated degree of freedom is called the world-line particle. The corresponding phase-space path-integral formula is given by

$$\begin{aligned} iW[\mathcal{A}] = \int_0^\infty \frac{ds}{s} e^{-\epsilon s} e^{-\frac{i}{2}M_{\text{eff}}^2 s} &\int_{x(0)=x(s)} \mathcal{D}x^\mu \mathcal{D}p_\mu \\ &\times \exp\left(\int_0^s d\tau[ip_\mu \dot{x}^\mu - iH(x, p; \mathcal{A})]\right), \end{aligned} \tag{100}$$

where we have imposed the boundary condition $x(0) = x(s)$ corresponding to the trace operation. Equation (100) gives a general path-integral formula for the generating functional in the world-line formalism. The applied background field is now interpreted as the gauge potential acting on the world-line particle. Thus, in the world-line formalism, the problem of evaluating the generating functional under the background field is translated into the quantum reflection problem with the corresponding potential.

In the present setup, the nonvanishing gauge field is $\mathcal{A}_0 = \frac{m}{2f_t^2} + \mu b(x^1 - x_{\text{ref}})$ and the other backgrounds are absent. As a result, the phase-space Lagrangian $L_H \equiv p_\mu \dot{x}^\mu - H(x, p; \mathcal{A})$ is given by

$$\begin{aligned} L_H = {}&p_0 \dot{x}^0 + p_1 \dot{x}^1 + p_{i,\perp} \dot{x}^{i,\perp} \\ &+ \frac{f_t^2}{2}\left(p_0 - \frac{m}{2f_t^2} - \mu b(x^1 - x_{\text{ref}})\right)^2 \\ &- \frac{f_s^2}{2}p_1^2 - \frac{f_s^2}{2}p_{i,\perp}^2. \end{aligned} \tag{101}$$

We can perform most of the path integral as follows. First, the path integral with respect to the perpendicular variables are trivialized; namely, after performing the $x^{i,\perp}$ integration, we obtain $p_{i,\perp} = \text{const}$, and performing the $p_{i,\perp}$

---

[6]In the case of charged particle production, the constant piece of $\mathcal{A}_0(x)$ does not affect the production rate because it is a gauge degree of freedom. However, the constant piece of $B(x)$ appearing in $\mathcal{A}_0(x)$ in Eq. (90) in the case of magnon production is physical and is used to tune the collinear ground state, although it does not affect the production rate.

integration just shifts the normalization. Similarly, the x^0 integration leads to $p_0 = $ const, but we keep the c-number p_0 integration here. In addition, we perform the p_1 integra-

tion and shift the p_0 integration. After all procedures, we eventually obtain the simplified formula for the generating functional,

$$iW[\mathcal{A}] = \mathcal{N}' L^{d-1} T \int_0^\infty \frac{ds}{s} e^{-\epsilon s} e^{-\frac{i}{2} M_{\text{eff}}^2 s} \int dp_0 \int_{x^1(0)=x^1(s)} \mathcal{D}x^1 \exp(i\mathcal{S}_{\text{wl}}[x^1; p_0]), \tag{102}$$

where we have defined the effective action for the world-line particle as

$$\mathcal{S}_{\text{wl}}[x^1; p_0] = \int_0^s dt \left[\frac{1}{2f_s^2} (\dot{x}^1)^2 + \frac{f_t^2}{2} (p_0 - \mu b x^1)^2 \right]. \tag{103}$$

Note that the value of the world-line action associated with the possible classical solution, or the so-called world-line instanton, controls the nonperturbative contribution to the generating functional. Thus, the remaining task is to evaluate the value of the classical action associated with the world-line instanton.

A direct way to evaluate the value of the classical action is to use the Hamilton-Jacobi equation with the help of the saddle-point approximation (recall that the solution of the Hamilton-Jacobi equation gives the value of the action). The Hamilton-Jacobi equation in the present setup is given by

$$\frac{\partial \mathcal{S}_{\text{wl}}}{\partial s} + H_{\text{wl}}(x^1, p_0, p_1, s) = 0 \quad \text{and} \quad p_1 = \frac{\partial \mathcal{S}_{\text{wl}}}{\partial x^1}, \tag{104}$$

where H_{wl} denotes the world-line Hamiltonian defined by

$$H_{\text{wl}} = \frac{f_s^2}{2} p_1^2 - \frac{f_t^2}{2} (p_0 - \mu b x^1)^2. \tag{105}$$

Note that the world-line action enjoys the proper-time translational invariance, and thus, the Hamiltonian takes a constant value as $H_{\text{wl}} = \mathcal{E}_{\text{wl}} = $ const. As a result, we can solve the energy equation with respect to p_1 as

$$p_1(x^1) = \pm \frac{1}{f_s} \sqrt{2[\mathcal{E}_{\text{wl}} + V_{\text{wl}}(p_0; x^1)]},$$

$$\text{with} \quad V_{\text{wl}}(p_0; x^1) \equiv \frac{f_t^2}{2} (p_0 - \mu b x^1)^2. \tag{106}$$

As a last step, we use the stationary phase condition for the proper time integral, which leads to $-M_{\text{eff}}^2/2 + \partial \mathcal{S}_{\text{wl}}/\partial s = 0$. By comparing this with the Hamilton-Jacobi equation, we find the value of the energy given by $\mathcal{E}_{\text{wl}} = -M_{\text{eff}}^2/2$. This indicates classical turning points, at which $\mathcal{E}_{\text{wl}} + V_{\text{wl}}(p_0; x^1)$ vanishes, appearing on the real axis $x^1 \in \mathbb{R}$. Then, corresponding classical solutions, satisfying the periodic boundary condition, has a pure imaginary momentum p_1, and thus, the proper time will also be pure imaginary.

Wrapping up these results, we find the solution of the Hamilton-Jacobi equation as

$$\mathcal{S}_{\text{wl}}(s) = -\mathcal{E}_{\text{wl}} s + \frac{1}{f_s} \oint dx^1 \, p_1(x^1)$$

$$= \frac{1}{2} M_{\text{eff}}^2 s + \frac{i\pi M_{\text{eff}}^2}{f_s f_t \mu b}, \tag{107}$$

where we have used $\mathcal{E}_{\text{wl}} = -M_{\text{eff}}^2/2$ and performed the contour integral to proceed to the second line. Recalling the definition of the effective mass, we eventually find the leading imaginary part of the generating functional given by

$$\text{Im}\, W[\mathcal{A}] \simeq \mathcal{N} T V \exp\left(-\frac{\pi}{f_s f_t \mu b} \left(M^2 + \frac{m^2}{4 f_t^2} \right) \right). \tag{108}$$

As expected, this agrees with the leading part of Schwinger's formula for the constant electric field $E_x = \mu b$ and the effective mass $M_{\text{eff}}^2 = M^2 + \frac{m^2}{4 f_t^2}$ with the corrections by the coefficients of time and space kinetic terms f_t and f_s. Note that the ratio of the low-energy coefficients m^2/f_t^2 appears in the formula. As a result, the magnon production rate for antiferromagnets $m^2 = 0$ gives the canonical Schwinger's formula with the mass M^2 associated to the energy gap of magnons while that for ferromagnets $m^2/f_t^2 \to \infty$ vanishes as $\text{Im}\, W[A] \to 0$. This reflects the absence of the pair production in the nonrelativistic systems (infinite effective mass limit). Our result Eq. (108) for ferrimagnets with a general value of m^2/f_t^2 gives the interpolation between relativistic and nonrelativistic charged scalar fields in terms of the ground-state decay rate.

C. Possible experimental detection via inverse spin Hall effect

Let us discuss a possible way to detect the Schwinger mechanism of magnons in experiments. The vital point here is that the Schwinger mechanism of magnons induces the finite spin current $J_{\text{spin}}^i \equiv J_{a=3}^i$ attached to the remaining SO(2) symmetry. Thus, one can experimentally confirm the magnon Schwinger mechanism by detecting the spin current in our setup.

A nice way to detect the spin current is available using an inverse spin Hall effect [89,90] (see e.g., Ref. [91] and references therein for a recent overview on the spin Hall effect). Let us consider the experimental setup schematically shown in Fig. 9, in which we attach our magnetic materials to a
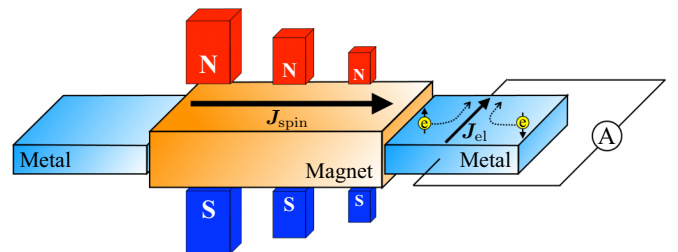

FIG. 9. A schematic picture of a way to detect the Schwinger mechanism of magnons using the inverse spin Hall effect.

nonmagnetic metal equipped with a large spin-orbit coupling such as Pt. Thanks to the inverse spin Hall effect, the spin current in magnetic materials induced by the inhomogeneous magnetic field can be converted to an electric current J_{el}^i in the attached nonmagnetic metal. Thus, by measuring the induced electric current (or voltage) in the metal, one can experimentally confirm the Schwinger mechanism of magnons taking place in magnetic materials.

We shall estimate the magnitude of the electric current signal by estimating that of the spin current. The spin current induced by the magnon Schwinger mechanism is proportional to the number of created magnon pairs, and thus proportional to the ground-state decay rate given in Eq. (108). In the same way with the electric current induced by the ordinary Schwinger mechanism, one can find the short-time behavior of the spin current generated by the magnon pair production as follows (see e.g., Ref. [92] in detail):

$$\langle J_{\mathrm{spin}}^{i=x}\rangle_{\mathcal{A}} = J_{\mathrm{pol}} + J_{\mathrm{cond}}, \quad \text{with}$$

$$J_{\mathrm{pol}} \simeq (\mu b)^{3/2} e^{-\frac{\pi}{f_s f_t \mu b}(M^2 + \frac{m^2}{4f_t^2})}\theta(t), \qquad (109)$$

$$J_{\mathrm{cond}} \simeq t(\mu b)^2 e^{-\frac{\pi}{f_s f_t \mu b}(M^2 + \frac{m^2}{4f_t^2})}\theta(t),$$

where we take $t = 0$ as the initial time, from which we start to apply the inhomogeneous magnetic field to the collinear ground state. The constant current J_{pol} describes a contribution coming from the pair production itself, while the linearly growing one J_{cond} does that from the accelerated motion of created magnons. In the band theory for electrons, J_{pol} and J_{cond} are called the interband current and intraband current, respectively. Thus, one possible experimental confirmation of the magnon Schwinger mechanism is to find the specific μb (the magnetic field gradient) dependence of the electric current in the attached metal. Note, however, that the linear growth of J_{pol} would saturate by considering (i) the size of sample magnets along the x direction and (ii) an effect of impurity scattering, which complicates the μb dependence in the experimental setup.

It is worth emphasizing an advantage in realizing the pair production of magnons compared to the Schwinger mechanism for electrons and positrons. The main experimental difficulty in detecting the ordinary Schwinger mechanism results from the fact that we need to apply electric fields that are too huge to find measurable effects. This is because the ground-state decay rate (or the induced electric current) is exponentially suppressed as $e^{-m_{\mathrm{el}}^2/eE}$ with the electron mass m_{el} and the applied electric field eE. Since the electron has a definite mass gap that we cannot control, it has still been impossible to experimentally realize such a huge electric field. In contrast, the magnon Schwinger mechanism is controlled by the gap of magnons, which could take a small value depending on magnetic materials [see Eqs. (108) and (109)]. If there is a magnet that has a small enough gap for magnons, it may be possible to detect the Schwinger mechanism more easily by applying the inhomogeneous magnetic field.

However, we also note that the typical magnetic material would have too large of a gap since it is controlled by the anisotropic potential resulting from the spin-orbit coupling. For instance, MnF_2 develops an antiferromagnetic order at a

low temperature (see e.g., Ref. [93]). The inelastic neutron scattering experiment [94] shows the gap for magnons is of order $\Delta \equiv M/f_t \sim 1$ meV with its propagating speed $c_s \equiv f_s/f_t \sim 60$ m/s. As a result, the critical value for the magnetic field gradient b_c, at which the dominant exponential factor in Eq. (109) becomes $O(1)$, is estimated as

$$\frac{\Delta^2}{c_s \mu b_c} \sim 1 \Leftrightarrow b_c \sim 10^9 \text{ T/cm} \quad \text{for } MnF_2, \qquad (110)$$

which is too difficult to achieve in experiments (we used $\mu = g\mu_B$ with the g-factor g and Bohr magneton μ_B). Therefore, we need to find a considerably symmetric antiferromagnet having a tiny gap (10^{-4} smaller than that of MnF_2) to detect the magnon pair production with the experimentally accessible size of magnetic fields. Another possible way to amplify the experimental signal is to apply a time-dependent magnetic-field gradient on the top of the constant one since it is known to enhance the pair production rate [95–101]. It is interesting to investigate such an enhancement mechanism for the magnon pair production, which is worth pursuing as a future study.

VI. DISCUSSION AND OUTLOOK

In this paper, we have developed a unified way to implement various SO(3) symmetry-breaking terms—the magnetic field, single-ion anisotropy, and DM interaction—into the low-energy EFT of spin systems. We have also applied the constructed effective Lagrangian to certain situations where the symmetry-breaking terms induce nontrivial dynamics. We have shown that two simple noncollinear ground states (helical and spiral phases) support the translational phonon as the resulting NG mode while they give a qualitatively different low-energy spectrum, such as isotropic versus anisotropic dispersion relations. The reason for this qualitative difference was clarified based on the symmetry-breaking pattern. We have also discussed the analog of the Schwinger mechanism by evaluating the decay rate of the collinear ground state induced by the inhomogeneous magnetic field.

While our formulation allows the symmetry-based systematic construction of the effective Lagrangian, we only consider its application in simplified setups, where the effect of the fluctuation is neglected. For example, in analyzing the helical/spiral phases, we have neglected the effect of the fluctuation resulting from, e.g., the quantum nature of systems and/or the gapless NG mode. In fact, our analysis to find the ground state is based on the tree-level (or mean-field level) discussion, which could be affected by the fluctuation already present in the nonlinear sigma model.

Also, the analysis on the Schwinger mechanism for magnons is performed in the theoretically idealized setup, where we assume the constant slope for the applied magnetic field. In experiments, it is easier to realize the magnetic field periodic in space and time. As we mentioned at the end of last section, this will also be useful in experimental detections of the magnon pair production since a time-dependent background field on the top of the constant one enhances the pair production rate [95–101]. Besides, applying magnetic fields periodic in time, realized by laser irradiation, is interesting in its own right because it could result in a higher-harmonics

generation even in magnets [102,103]. The analysis of such a more realistic and interesting situation is strongly desirable.

Throughout the analysis in Secs. III–V, we rely on the continuum field theoretical description of spin systems. Since the underlying model is composed of spins living on the lattice, there could be a potential deviation due to our continuum approximation. However, such a deviation would not drastically affect the main result of the present paper because the deviation appears in the large momentum regime while we mainly discuss physics at the low momentum. For example, we focus on the low-energy spectrum of the gapless excitations in Sec. IV, which is protected by the symmetry-breaking pattern thanks to the NG theorem. Our formula for the magnon Schwinger mechanism is also expected to be robust because the dominant contribution to the pair production rate comes from the low-momentum region[7] of order of the energy gap Δ. In fact, one finds the finite momentum contribution is exposed to a further exponential suppression. This implies that the low-momentum region, where the corresponding frequency $\omega(\boldsymbol{k})$ satisfies, e.g., $\omega(\boldsymbol{k}) \lesssim 2\Delta$, controls the pair production rate. Thus, our field theoretical approach gives a good approximation if the energy spectrum around $\omega(\boldsymbol{k}) \lesssim 2\Delta$ is well approximated.

There are also other several interesting prospects based on the present paper. One direction is to investigate various transport phenomena in spin systems by extending our effective Lagrangian approach. For instance, despite the experimental realization of the thermal Hall effect in spin systems, its field-theoretical description has still been unclear. Our formulation has a potential advantage to provide a direct connection between the EFT and the underlying lattice descriptions of spin systems. However, it is necessary to relax our assumption on the cubic-type lattice since the thermal Hall effect takes place in different types of the lattice structure (see e.g., Ref. [104]). Generalization to such a nontrivial lattice may be important to study the thermal Hall effect based on the EFT. Besides, it is also interesting to investigate the transport phenomena of spin densities in detail, which lead to a potential connection to the spintronics (see, e.g., Ref. [105] for a review). While the presence of small explicit breaking terms makes total spins as approximate conserved charges, its dynamics is a primary concern of the spintronics. For example, a recent proposal in Ref. [106] for a mechanical generation of the DM interaction and the resulting spin current is an interesting problem. It is worthwhile developing the effective Lagrangian approach to the spintronics (see also Refs. [107,108] for reviews discussing the effective Lagrangian approach to the spintronics).

Another interesting direction is to clarify a possible realization and resulting dynamics of the magnetic skyrmion

based on the EFT.[8] In $(2 + 1)$-dimensional cases, the magnetic skyrmion represents a nontrivial topologically stable configuration of the magnetization vector, which results in the topologically conserved charge. As is the case for the skyrmion in hadron physics [109–111], it is worth understanding what conserved quantity this charge describes. A natural candidate (for, at least, particular spin systems) is the electric charge attached to the underlying charge carrier like an itinerant electron. In such systems, when the ground state supports the finite local skyrmion charge (like the spiral phase or skyrmion crystal), there should be an induced electromagnetic field [36,112]. Thus, the spin could affect the dynamics of the electromagnetic field through its topological configuration, although it is not an electrically charged object. This implies a possibility of the interesting coupled dynamics of the spin and dynamical electromagnetism in a similar manner with the charge density wave phase of many-electron systems. We leave these interesting problems as future works.

APPENDIX: EFFECTIVE LAGRANGIAN FROM COSET CONSTRUCTION

In this Appendix, we provide another way to construct the effective Lagrangian Eq. (20); that is, the coset construction originally developed in the context of the high-energy physics [113–115] and recently applied to magnons in Ref. [38]. We assume that the DM interaction is weaker than the potential; e.g.,

$$\left(\kappa_i^a\right)^2 \ll W, B. \tag{A1}$$

This assumption allows us to start exploring the background (ground state) as a collinear state with the symmetry-breaking pattern dictated by the potential and to use the resulting effective Lagrangian to examine the effect of the DM interaction.

Suppose that the collinear ground state of the spin system Eq. (1) spontaneously breaks the approximate SO(3) symmetry down to SO(2). We are interested in the low-energy

---

[7]Of course, there is a problem whether the magnetic material would be stable or not under the applied magnetic field gradient. However, once we find such a stable material with a tiny gap, the field theoretical approach will give a good description for the magnon pair production.

[8]The effective field theories and NG modes in the presence of a single magnetic skyrmion line [122] and a single magnetic domain wall [77] were discussed in the absence of the DM term.

(long wavelength) behavior of the system, and we can directly employ the field-theoretical (continuum) description of the associated pseudo-NG mode. Thus, we have the background fields A_μ^a and W transforming as the SO(3) gauge and matter field, respectively, as discussed in the main text. The main difference is that we assume the symmetry-breaking pattern, which allows us to directly introduce the NG field in the coset construction.

Let us now review how the magnon (NG field) is introduced in the effective Lagrangian [38]. First, we divide the generators of the SO(3) Lie algebra $t_a = \{t_\alpha, t_3\}$ belonging to the broken part indices $\alpha = 1, 2$ and unbroken SO(2) index $a = 3$ satisfying

$$\mathrm{tr}(t_\alpha t_3) = 0, \quad \mathrm{tr}(t_\alpha t_\beta) = g_{\alpha\beta}, \quad \mathrm{tr}(t_3 t_3) = g_{33}, \quad \text{(A2)}$$

with the Cartan metric g_{ab}, which reduces to $g_{ab} \to 2\delta_{ab}$ if we choose Eqs. (10). The basic ingredient is the coset $\xi(\pi) \in \mathrm{SO}(3)/\mathrm{SO}(2)$ parametrizing the NG modes, or the magnons π^α, whose representative is, e.g., parametrized by

$$\xi(\pi) = e^{i\pi}, \quad \pi \equiv \pi^\alpha t_\alpha, \quad \text{(A3)}$$

using the explicit form given in Eqs. (10). We note that the local $g(x) \in \mathrm{SO}(3)$ transformation, by definition, acts on the (right-)coset element $\xi(\pi)$ as

$$\xi(\pi) \to \xi(\pi') = g(x)\xi(\pi)h^{-1}(\pi, g(x)), \quad \text{(A4)}$$

with $h(\pi, g(x)) \in \mathrm{SO}(2)$. We then introduce the gauged Maurer-Cartan one-form $\alpha_\mu(\pi)$ as

$$\alpha_\mu(\pi) \equiv i^{-1}\xi^{-1}(\pi)D_\mu\xi(\pi). \quad \text{(A5)}$$

Here, we defined the covariant derivative of the coset,

$$D_\mu\xi(\pi) \equiv \partial_\mu\xi(\pi) - iA_\mu(x)\xi(\pi), \quad \text{(A6)}$$

with the background SO(3) gauge field $A_\mu = A_\mu^a t_a$, whose transformation rule is given in Eq. (15). With a help of Eqs. (15) and (A4), we can show that the transformation rules for projected components of the Maurer-Cartan one-form $\alpha_{\mu\parallel} \equiv \frac{1}{2}\mathrm{tr}(\alpha_\mu t_3)t_3$ and $\alpha_{\mu\perp} \equiv \frac{1}{2}\sum_\alpha \mathrm{tr}(\alpha_\mu t_\alpha)t_\alpha$ are given by

$$\begin{aligned} \alpha_{\mu\parallel}(\pi) \to \alpha_{\mu\parallel}(\pi') &= h(\pi, g(x))\alpha_{\mu\parallel}(\pi)h^{-1}(\pi, g(x)) \\ &\quad + i^{-1}h(\pi, g(x))\partial_\mu h^{-1}(\pi, g(x)), \\ \alpha_{\mu\perp}(\pi) \to \alpha_{\mu\perp}(\pi') &= h(\pi, g(x))\alpha_{\mu\perp}(\pi)h^{-1}(\pi, g(x)). \end{aligned} \quad \text{(A7)}$$

The Maurer-Cartan one-form describes the NG field (magnons), which is an alternative to the normalized vector n^a.

We have elucidated the transformation rules of the Maurer-Cartan one-form and background fields in Eqs. (15), (A4), and (A7). Then, we can systematically construct the general effective Lagrangian once we fix the power counting scheme. As usual, space-time derivatives of the NG field $\pi^\alpha(x)$ results in higher-order contributions to the low-energy EFT. We thus consider the leading-order effective Lagrangian up

to terms with second-order derivatives of $\pi^\alpha(x)$. This motivates us to count background fields as $A_\mu^a = O(\partial_\mu)$ and $W = O(\partial_i^2)$. Summarizing these, we will employ the power-counting scheme,

$$\pi^\alpha = O(\partial_\mu^0), \quad A_\mu^a = O(\partial_\mu), \quad W = O(\partial_i^2), \quad \text{(A8)}$$

to construct the leading-order effective Lagrangian.

By the use of the above transformation rule and power-counting scheme, we are able to write the most general SO(3)-invariant effective Lagrangian for magnons. Here, it is important to notice that the spin system under consideration does not respect the Lorentz symmetry, which means that time and spatial components of $\alpha_{\mu\perp}$ can appear independently. We thus immediately find invariant terms $\mathrm{tr}(\alpha_{0\perp}\alpha_{0\perp})$ and $\delta^{ij}\mathrm{tr}(\alpha_{i\perp}\alpha_{j\perp})$ respecting the spatial rotation symmetry. Furthermore, noting that the unbroken SO(2) symmetry is Abelian, we find an additional invariant term $\mathrm{tr}(t_3\alpha_{0\parallel})$. This can be explicitly shown that the general parametrization $h(\pi, g(x)) = e^{ip(\pi, g(x))t_3}$ leads to $h\partial_\mu h^{-1} = -it_3\partial_\mu p(\pi, x)$, which means $\mathrm{tr}(t_3\alpha_{0\parallel})$ is invariant up to a surface term. In addition, a combination of the coset $\xi(x)$ and the background field $W(x)$ generates another invariant term. Thanks to the relation $\mathrm{tr}(\xi^{-1}W\xi) = \mathrm{tr}\,W = \mathrm{const}$, we need to keep only one of two invariant terms $(\xi^{-1}W\xi)^{33}\delta_{\alpha\beta}$ and $(\xi^{-1}W\xi)^{\alpha\beta}$, where indices denote that for the matrix.[9] In short, we have four independent invariant terms composed of the gauged Maurer-Cartan one-form:

$$\mathrm{tr}(\alpha_{0\perp}\alpha_{0\perp}), \quad \delta^{ij}\mathrm{tr}(\alpha_{i\perp}\alpha_{j\perp}), \quad \mathrm{tr}(t_3\alpha_{0\parallel}), \quad (\xi^{-1}W\xi)^{33}. \quad \text{(A9)}$$

Taking account of all these, we write down the general SO(3)-invariant effective Lagrangian of magnons in the leading-order derivative expansion (up to two derivatives) as

$$\begin{aligned} \mathcal{L}_{\mathrm{eff}}^{(2)} = &-\frac{m}{2}\mathrm{tr}(t_3\alpha_{0\parallel}) + \frac{f_t^2}{4}\mathrm{tr}(\alpha_{0\perp}\alpha_{0\perp}) \\ &-\frac{f_s^2}{4}\mathrm{tr}(\alpha_{i\perp}\alpha_{i\perp}) + r(\xi^{-1}W\xi)^{33}. \end{aligned} \quad \text{(A10)}$$

Since the coset representative $\xi(\pi) = e^{i\pi}$ contains an infinite number of the magnon field $\pi^\alpha(x)$, this effective Lagrangian describes the fully interacting model of magnons. By expanding the coset representative $\xi(\pi) = e^{i\pi}$, we obtain the effective Lagrangian Eq. (20) in the main text. One sees that four low-energy coefficients attached to four invariants in Eq. (A9) indeed coincide with those appearing in the O(3) nonlinear sigma model. As discussed in the main text, their matching condition are given in Eqs. (27) and (28).

---

[9]There seems to be another invariant term, $\mathrm{tr}(t_3\xi^{-1}W\xi)$. However, this term with its complex conjugate will vanish, and thus does not appear in the effective Lagrangian.

[1] Y. Nambu and G. Jona-Lasinio, Phys. Rev. **122**, 345 (1961).

[2] J. Goldstone, Nuovo Cim. **19**, 154 (1961).

[3] J. Goldstone, A. Salam, and S. Weinberg, Phys. Rev. **127**, 965 (1962).

[4] P.-G. De Gennes, J. Phys. Colloq. **30**, C4 (1969).

[5] P.-G. De Gennes and J. Prost, *The Physics of Liquid Crystals* (Oxford University Press, Oxford, 1993), Vol. 83.

[6] P. M. Chaikin and T. C. Lubensky, *Principles of Condensed Matter Physics* (Cambridge University Press, Cambridge, 2000).

[7] P. Fulde and R. A. Ferrell, Phys. Rev. **135**, A550 (1964).

[8] A. Larkin and Y. Ovchinnikov, Zh. Eksp. Teor. Fiz. **47**, 1136 (1964).

[9] A. Larkin and Y. Ovchinnikov, Sov. Phys. JETP **20**, 762 (1965).

[10] H. B. Nielsen and S. Chadha, Nucl. Phys. B **105**, 445 (1976).

[11] H. Leutwyler, Phys. Rev. D **49**, 3033 (1994).

[12] V. A. Miransky and I. A. Shovkovy, Phys. Rev. Lett. **88**, 111601 (2002).

[13] T. Schafer, D. T. Son, M. A. Stephanov, D. Toublan, and J. J. M. Verbaarschot, Phys. Lett. B **522**, 67 (2001).

[14] Y. Nambu, J. Stat. Phys. **115**, 7 (2004).

[15] T. Brauner, Symmetry **2**, 609 (2010).

[16] H. Watanabe and T. Brauner, Phys. Rev. D **84**, 125013 (2011).

[17] Y. Hidaka, Phys. Rev. Lett. **110**, 091601 (2013).

[18] H. Watanabe and H. Murayama, Phys. Rev. Lett. **108**, 251602 (2012).

[19] A. Nicolis and F. Piazza, Phys. Rev. Lett. **110**, 011602 (2013), [Addendum: **110**, 039901(E) (2013)].

[20] H. Watanabe and H. Murayama, Phys. Rev. X **4**, 031057 (2014).

[21] D. A. Takahashi and M. Nitta, Ann. Phys. **354**, 101 (2015).

[22] J. O. Andersen, T. Brauner, C. P. Hofmann, and A. Vuorinen, J. High Energy Phys. 08 (2014) 088.

[23] T. Hayata and Y. Hidaka, Phys. Rev. D **91**, 056006 (2015).

[24] A. J. Beekman, L. Rademaker, and J. van Wezel, SciPost Phys. Lect. Notes, 11 (2019).

[25] H. Watanabe, Ann. Rev. Condensed Matter Phys. **11**, 169 (2020).

[26] E. Ivanov and V. Ogievetsky, Teor. Mat. Fiz. **25**, 164 (1975).

[27] I. Low and A. V. Manohar, Phys. Rev. Lett. **88**, 101602 (2002).

[28] H. Watanabe and H. Murayama, Phys. Rev. Lett. **110**, 181601 (2013).

[29] A. Nicolis, R. Penco, F. Piazza, and R. A. Rosen, J. High Energy Phys. 11 (2013) 055.

[30] T. Hayata and Y. Hidaka, Phys. Lett. B **735**, 195 (2014).

[31] T. Brauner and H. Watanabe, Phys. Rev. D **89**, 085004 (2014).

[32] Y. Hidaka, T. Noumi, and G. Shiu, Phys. Rev. D **92**, 045020 (2015).

[33] C. Burgess, Phys. Rep. **330**, 193 (2000).

[34] J. M. Román and J. Soto, Int. J. Mod. Phys. B **13**, 755 (1999).

[35] C. P. Hofmann, Phys. Rev. B **60**, 388 (1999).

[36] O. Bar, M. Imboden, and U. J. Wiese, Nucl. Phys. B **686**, 347 (2004).

[37] F. Kampfer, M. Moser, and U.-J. Wiese, Nucl. Phys. B **729**, 317 (2005).

[38] S. Gongyo, Y. Kikuchi, T. Hyodo, and T. Kunihiro, Prog. Theor. Exp. Phys. **2016**, 083B01 (2016).

[39] I. Dzyaloshinsky, J. Phys. Chem. Solids **4**, 241 (1958).

[40] T. Moriya, Phys. Rev. **120**, 91 (1960).

[41] Y. Togawa, T. Koyama, K. Takayanagi, S. Mori, Y. Kousaka, J. Akimitsu, S. Nishihara, K. Inoue, A. S. Ovchinnikov, and J. Kishine, Phys. Rev. Lett. **108**, 107202 (2012).

[42] J.-i. Kishine and A. Ovchinnikov, *Solid State Physics* (Elsevier, Amsterdam, 2015), Vol. 66, pp. 1–130.

[43] Y. Togawa, Y. Kousaka, K. Inoue, and J.-i. Kishine, J. Phys. Soc. Jpn. **85**, 112001 (2016).

[44] S. Mühlbauer, B. Binz, F. Jonietz, C. Pfleiderer, A. Rosch, A. Neubauer, R. Georgii, and P. Böni, Science **323**, 915 (2009).

[45] X. Yu, Y. Onose, N. Kanazawa, J. Park, J. Han, Y. Matsui, N. Nagaosa, and Y. Tokura, Nature (London) **465**, 901 (2010).

[46] S. Heinze, K. Von Bergmann, M. Menzel, J. Brede, A. Kubetzka, R. Wiesendanger, G. Bihlmayer, and S. Blügel, Nat. Phys. **7**, 713 (2011).

[47] N. Nagaosa and Y. Tokura, Nat. Nanotechnol. **8**, 899 (2013).

[48] E. B. Bogomolny, Sov J. Nucl. Phys. **24**, 449 (1976).

[49] M. K. Prasad and C. M. Sommerfield, Phys. Rev. Lett. **35**, 760 (1975).

[50] B. Barton-Singer, C. Ross, and B. J. Schroers, Commun. Math. Phys. **375**, 2259 (2020).

[51] C. Adam, J. M. Queiruga, and A. Wereszczynski, J. High Energy Phys. 07 (2019) 164.

[52] C. Adam, K. Oles, T. Romanczukiewicz, and A. Wereszczynski, arXiv:1902.07227.

[53] B. Schroers, SciPost Phys. **7**, 030 (2019).

[54] C. Ross, N. Sakai, and M. Nitta, J. High Energy Phys., 02 (2021) 095.

[55] M. Hongo, T. Fujimori, T. Misumi, M. Nitta, and N. Sakai, Phys. Rev. B **101**, 104417 (2020).

[56] J. H. Han, J. Zang, Z. Yang, J.-H. Park, and N. Nagaosa, Phys. Rev. B **82**, 094429 (2010).

[57] M. Kataoka, J. Phys. Soc. Jpn. **56**, 3635 (1987).

[58] S. V. Maleyev, Phys. Rev. B **73**, 174402 (2006).

[59] J.-i. Kishine and A. S. Ovchinnikov, Phys. Rev. B **79**, 220405(R) (2009).

[60] S. Toth and B. Lake, J. Phys.: Condens. Matter **27**, 166002 (2015).

[61] R. Yadav, M. Pereiro, N. A. Bogdanov, S. Nishimoto, A. Bergman, O. Eriksson, J. van den Brink, and L. Hozoi, Phys. Rev. Mater. **2**, 074408 (2018).

[62] D. Belitz, T. R. Kirkpatrick, and A. Rosch, Phys. Rev. B **73**, 054431 (2006).

[63] L. Radzihovsky and T. C. Lubensky, Phys. Rev. E **83**, 051701 (2011).

[64] M. Garst, J. Waizner, and D. Grundler, J. Phys. D **50**, 293002 (2017).

[65] F. Sauter, Z. Phys. **69**, 742 (1931).

[66] W. Heisenberg and H. Euler, Z. Phys. **98**, 714 (1936).

[67] V. Weisskopf, Kong. Dans. Vid. Selsk. Math-fys. Medd. **XIV** No. 6 (1936).

[68] J. S. Schwinger, Phys. Rev. **82**, 664 (1951).

[69] L. D. Landau, Phys. Z. Sowjetunion **2**, 46 (1932).

[70] C. Zener, Proc. Roy. Soc. Lond. A **137**, 696 (1932).

[71] E. C. G. Stueckelberg, Helv. Phys. Acta **5**, 369 (1932).

[72] E. Majorana, Nuovo Cim. **9**, 43 (1932).

[73] J. Kogut and L. Susskind, Phys. Rev. D **11**, 395 (1975).

[74] T. A. Kaplan, Z. Phys. B **49**, 313 (1983).

[75] L. Shekhtman, O. Entin-Wohlman, and A. Aharony, Phys. Rev. Lett. **69**, 836 (1992).

[76] F. Bloch, Z. Phys. **52**, 555 (1929).

[77] M. Kobayashi and M. Nitta, Phys. Rev. Lett. **113**, 120403 (2014).

[78] N. D. Mermin and H. Wagner, Phys. Rev. Lett. **17**, 1133 (1966).

[79] P. C. Hohenberg, Phys. Rev. **158**, 383 (1967).

[80] S. R. Coleman, Commun. Math. Phys. **31**, 259 (1973).

[81] M. Kobayashi and M. Nitta, Phys. Rev. D **92**, 045028 (2015).

[82] F. Gelis and N. Tanji, Prog. Part. Nucl. Phys. **87**, 1 (2016).

[83] R. Feynman, Phys. Rev. **80**, 440 (1950).

[84] R. P. Feynman, Phys. Rev. **84**, 108 (1951).

[85] V. Fock, Phys. Z. Sowjetunion **12**, 404 (1937).

[86] Y. Nambu, Prog. Theor. Phys. **5**, 82 (1950).

[87] C. Schubert, Phys. Rep. **355**, 73 (2001).

[88] G. V. Dunne and C. Schubert, Phys. Rev. D **72**, 105004 (2005).

[89] M. I. Dyakonov and V. Perel, JETP Lett. **13**, 467 (1971).

[90] M. I. Dyakonov and V. Perel, Phys. Lett. A **35**, 459 (1971).

[91] J. Sinova, S. O. Valenzuela, J. Wunderlich, C. H. Back, and T. Jungwirth, Rev. Mod. Phys. **87**, 1213 (2015).

[92] N. Tanji, Ann. Phys. **324**, 1691 (2009).

[93] S. M. Rezende, A. Azevedo, and R. L. Rodríguez-Suárez, J. Appl. Phys. **126**, 151101 (2019).

[94] S. Bayrakci, T. Keller, K. Habicht, and B. Keimer, Science **312**, 1926 (2006).

[95] W. Franz, Z. Naturforsch. A **13**, 484 (1958).

[96] L. V. Keldysh, Sov. Phys. JETP **7**, 788 (1958).

[97] R. Schutzhold, H. Gies, and G. Dunne, Phys. Rev. Lett. **101**, 130404 (2008).

[98] A. Di Piazza, E. Lotstedt, A. I. Milstein, and C. H. Keitel, Phys. Rev. Lett. **103**, 170403 (2009).

[99] G. V. Dunne, H. Gies, and R. Schützhold, Phys. Rev. D **80**, 111301(R) (2009).

[100] H. Taya, Phys. Rev. D **99**, 056006 (2019).

[101] H. Taya, Phys. Rev. Research **2**, 023257 (2020).

[102] S. Takayoshi, Y. Murakami, and P. Werner, Phys. Rev. B **99**, 184303 (2019).

[103] T. N. Ikeda and M. Sato, Phys. Rev. B **100**, 214424 (2019).

[104] H. Katsura, N. Nagaosa, and P. A. Lee, Phys. Rev. Lett. **104**, 066403 (2010).

[105] S. Maekawa, S. O. Valenzuela, T. Kimura, and E. Saitoh, *Spin Current* (Oxford University Press, 2017), Vol. 22.

[106] J. Fujimoto and M. Matsuo, Phys. Rev. B **102**, 020406(R) (2020).

[107] G. Tatara, H. Kohno, and J. Shibata, Phys. Rep. **468**, 213 (2008).

[108] G. Tatara, Physica E: Low Dimens. Syst. Nanostruct. **106**, 208 (2019).

[109] T. H. R. Skyrme, Proc. R. Soc. Lond. A **260**, 127 (1961).

[110] T. H. R. Skyrme, Nucl. Phys. **31**, 556 (1962).

[111] E. Witten, Nucl. Phys. B **160**, 57 (1979).

[112] U. J. Wiese, Nucl. Phys. Proc. Suppl. **141**, 143 (2005).

[113] S. R. Coleman, J. Wess, and B. Zumino, Phys. Rev. **177**, 2239 (1969).

[114] C. G. Callan, Jr., S. R. Coleman, J. Wess, and B. Zumino, Phys. Rev. **177**, 2247 (1969).

[115] M. Bando, T. Kugo, and K. Yamawaki, Phys. Rep. **164**, 217 (1988).

[116] M. Pereiro, D. Yudin, J. Chico, C. Etz, O. Eriksson, and A. Bergman, Nat. Commun. **5**, 4815 (2014).

[117] K. V. Shanavas and S. Satpathy, Phys. Rev. B **93**, 195101 (2016).

[118] K. Ohashi, T. Fujimori, and M. Nitta, Phys. Rev. A **96**, 051601(R) (2017).

[119] D. A. Takahashi, K. Ohashi, T. Fujimori, and M. Nitta, Phys. Rev. A **96**, 023626 (2017).

[120] T. Fujimori, M. Nitta, and K. Ohashi, Prog. Theor. Exp. Phys. **2020**, 053B01 (2020).

[121] L. Radzihovsky, Phys. Rev. A **84**, 023611 (2011).

[122] M. Kobayashi and M. Nitta, Phys. Rev. D **90**, 025010 (2014).